Renewable and Sustainable Energy Reviews 109 (2019) 138–159

Contents lists available at ScienceDirect

Renewable and Sustainable Energy Reviews

journal homepage: www.elsevier.com/locate/rser

Critical review of non-invasive diagnosis techniques for quantification of degradation modes in lithium-ion batteries

Carlos Pastor-Fernández[a,*], Tung Fai Yu[b], W. Dhammika Widanage[a], James Marco[a]

[a] WMG, University of Warwick, Coventry, CV4 7AL UK
[b] Jaguar Land Rover, Banbury Road, Warwick, CV35 0XJ UK

ARTICLE INFO

Keywords:
Lithium ion technology
Battery health diagnosis
Degradation modes
Critical and systematic review

ABSTRACT

Understanding the root causes of Lithium-ion battery degradation is a challenging task due to the complexity of the different mechanisms involved. For simplicity, ageing mechanisms are often grouped into three degradation modes (DMs): conductivity loss, loss of active material and loss of lithium inventory. Battery Management Systems (BMSs) do not currently include an indication of the underlying DMs causing the degradation. Pseudo Open Circuit Voltage (pOCV), Incremental Capacity - Differential Voltage (IC-DV), Electrochemical Impedance Spectroscopy and Differential Thermal Voltammetry are the most common non-invasive diagnosis techniques studied in the literature to quantify DMs. This work presents a critical and systematic review of these techniques with the focus on the elaboration of their strengths and weaknesses for the implementation in automotive applications. Firstly, each technique is classified into different groups and their working principles are presented. Secondly, an evaluation criterion is introduced to review each technique following a systematic approach. The comparison of the techniques highlight that pOCV and IC-DV are the most advantageous because they fulfill most of the points included in the evaluation criteria. The further implementation of these techniques would support battery lifetime control strategies and battery designs.

1. Introduction

Hybridization and electrification of vehicle propulsion systems have become more critical in recent years because of two main factors. Firstly, they contribute to increasing the total vehicle's efficiency; and secondly, they can eliminate the vehicle's greenhouse emissions [1]. Currently, Lithium-ion Batteries (LIBs) are considered to be a highly prospective technology in this industry due to their higher specific or volumetric power and energy density and high cycle lifetime in comparison to other technologies such as lead-acid or nickel-metal hydride [1].

The Battery Management System (BMS) is a software and hardware unit which, among other functions, monitors battery ageing to ensure and guarantee safety, performance and battery longevity. It is widely known that continuous degradation of LIBs has a negative impact in battery's performance and range prediction [2,3]. Continuous and severe degradation can even trigger catastrophic battery failures causing larger economical losses affecting the battery industry and manufacturer's reputation [4]. Hence, it is essential to understand and limit the causes of LIB's degradation.

Degradation of LIBs is an extremely complex process that depends on a variety of ageing mechanisms. Ageing mechanisms can be caused by parasitic reactions such as Solid Electrolyte Interphase (SEI) or lithium plating [5]; or can be caused by mechanical degradation (e.g., phase changes) or mechanical stress (e.g., particle cracking) [6]. Ageing mechanisms are accelerated by extrinsic and intrinsic factors [7]. Extrinsic factors are given by the inhomogeneous operating conditions that a cell can be subject to, e.g., accessible temperature gradients due to thermal management's constraints [7]. These factors can be minimised by controlling the parameters which drive the dynamics of the battery and are affected by the operating conditions (e.g., temperature, C-rate, state of charge (SoC) or Depth of Discharge (DoD)) [1]. Intrinsic factors are inherent to inconsistent manufacturing processes, e.g., variations in cell quality within cells and can be limited by improving quality control and manufacturing processes [8].

The BMS usually quantifies battery State of Health (SoH) based on the decrease in capacity (SoH_E) and increase in resistance (SoH_P), metrics that are directly related to the vehicle range and power capability, respectively [9]. The BMS has access to simple measurements such as voltage, current and temperature, and hence, monitoring the ageing mechanisms in real-time conditions becomes a challenging task. Previous studies [10–12] suggest categorising the different ageing

* Corresponding author.
E-mail address: carlos.pastor@warwick.ac.uk (C. Pastor-Fernández).

https://doi.org/10.1016/j.rser.2019.03.060
Received 2 August 2018; Received in revised form 28 March 2019; Accepted 29 March 2019
Available online 17 April 2019

mechanisms into three degradation modes (DMs) called conductivity loss (CL), loss of active material (LAM) and loss of lithium inventory (LLI). This classification would allow a BMS to indicate the ageing root causes in real-time applications. This approach will underpin the development of novel control strategies to maximise battery life as well as the improvement of battery designs [3]. In our previous article [13], the capability to identify and quantify DMs using Incremental Capacity-Differential Voltage (IC-DV) and Electrochemical Impedance Spectroscopy (EIS) was studied. Other authors have presented alternative methods based on non-invasive diagnosis techniques such as pseudo Open Circuit Voltage (pOCV) [10,14–16], Differential Thermal Voltammetry (DTV) [17–19] or a combination of pOCV and EIS techniques [20]. Each of these methods follows an automated process that can be implemented in real-world applications. In this article, real-world applications can be on-board and off-board. On-board processes take place uniquely inside the vehicle through a microcontroller unit (MCU). Off-board operations require the use of external equipment to process the parameters. On-board and off-board are different terms than online and offline. On-board and off-board determine whether data is processed internally or externally with respect to the vehicle (where the data is processed). Online and offline denote when data is being processed. Offline processing is when a method is applied retroactively, on data which has been previously acquired. Online processing is when a method is applied in real time, as soon as the data is being acquired. There is also a combination of offline and online options, called hybrid option. The hybrid option is when some parameters are processed offline and others online. Based on this, Table 1 shows the different possibilities for an on-board and an off-board process.

A comparative review of non-invasive DMs diagnosis techniques has never been conducted. The majority of the reviews focus on studying SoH diagnosis [1,21–24] or prognosis [25–28] techniques in isolation without considering the quantification of DMs. This study aims to systematically evaluate the relative merits of the techniques that are capable to identify and quantify DMs non-invasively. It is beyond the scope of this study to review invasive diagnostic techniques such as Scanning Electron Microscopy (SEM), Energy Dispersive Spectrometry (EDS) or X-Ray Diffractometry (XRD). These post-mortem techniques are not considered in this review because they require opening up the cells. This characteristic consequently makes their application in real-world scenarios unfeasible. Non-invasive diagnostic techniques are reviewed according to the requirements that these techniques need to fulfill as part of a Battery Electric Vehicle (BEV) application. The outcomes of this review will support the selection of the most appropriate non-invasive diagnostic technique to quantify DMs.

The structure of this work is divided as follows: Section 2 describes the nature of the ageing mechanisms involved in LIBs. The working principles of the diagnostic techniques suitable for non-invasive identification and quantification of DMs are described in Section 3. These techniques are subsequently reviewed in Section 5 following the evaluation criterion described in Section 4. This criterion is derived according to the requirements that a diagnostic method needs to fulfill in real-world automotive applications. Section 6 describes the limitations of this work, outlining areas that need to be further investigated. Finally, Section 7 presents the main conclusions of this study.

Table 1
Possibilities for on-board and off-board process.

Possibility	Process	Data processing
1	Off-board	Offline
2		Online
3		Hybrid
4	On-board	Offline
5		Online
6		Hybrid

2. Degradation mechanisms in lithium-ion batteries

Previously, studies [10–12,29] suggest categorising the different ageing mechanisms into DMs (CL, LLI and LAM). CL includes the degradation of the electronic parts of the battery such as current collector corrosion or binder decomposition [5]. LLI is attributed to the variation of the number of lithium-ions (Li-ions) that are available for intercalation and de-intercalation processes [5]. LAM is related to structural transformations in the active material (positive or negative electrodes), and non-active material elements (separator and electrolyte) [5]. Fig. 1 illustrates the most pertinent ageing mechanisms which fall into a particular degradation mode. Each DM can lead to an increase in resistance (e.g., charge transfer or diffusion), a reduction in current density, capacity or/and power in a partly reversible (e.g., lithium plating) or irreversible (e.g., SEI formation) manner [30]. Uddin et al. [30] suggested a general relationship between battery ageing extrinsic factors (temperature, C-rate, SoC, ΔDoD and cycle number) and the affected component (positive or negative electrode) with the corresponding ageing mechanism and potential effects on LIBs. Following on from Uddin et al. [30], Table 2 suggests a generic relationship between battery extrinsic factors (temperature, C-rate, SoC, ΔDoD and cycle number) and the affected component (positive or negative electrode) with the corresponding ageing mechanism, most pertinent DM (LLI, LAM or CL), mechanism type (gradual, progressive degradation, or overstress, abrupt degradation) and most pertinent observed effects (Capacity Fade - CF, or/and Power Fade - PF). Previous studies that have examined the ageing mechanisms within LIBs [5,31] were also considered to reinforce this relationship further.

It is noteworthy that some ageing mechanisms are driven when two or more extrinsic factors co-occur. For instance, lithium plating is pertinent when the battery is cycled with high C-rates at low temperatures [5]. It is beyond the scope of this article to explain these ageing mechanisms at a material and chemical level. Further explanation regarding these degradation mechanisms can be found in a number of research publications such as [5,33,34]. The general ageing mechanisms presented in Table 2 hold true for most LIBs. Nonetheless, there might be pronounced differences for each particular LIB when taking into account the effect of having different cathode electrode materials (e.g., LFP, NCA or NMC) or form factors (e.g., cylindrical, pouch or prismatic). The reader is referred to previous publications such as [33,35] where the degradation mechanisms are explained in greater detail according to the type of cathode material and form factor used.

3. Description of methods to identify and quantify DMs

LIB operation is characterised through two phenomena: thermodynamics (equilibrium) and kinetics (non-equilibrium) [36]. The diagnostic techniques reviewed in this study follow either thermodynamic or kinetic principles. The thermodynamic diagnostic techniques infer ageing mechanisms based on voltage phase changes. The kinetic techniques relate ageing mechanisms based on charge-transfer and diffusion reactions. It is noteworthy that the thermodynamic-based techniques consider some kinetics because it is not possible to charge/discharge the cells with zero current or absolute equilibrium state [10]. This amount of kinetics is assumed to be negligible throughout the thermodynamic-based techniques given that the current employed is typically very low, e.g., in the order of C/10 or C/25.

As thermodynamics and kinetics involve different electrochemical processes, the insights that can be obtained through a thermodynamic or kinetic method can be different. This conclusion motivates the research of combining both types of methods to achieve a more complete diagnosis of the battery. Fig. 2 shows the measurements the BMS needs in order to deploy the diagnostic techniques reviewed. The pOCV is measured during charging or discharging a battery at low C-rates (C-

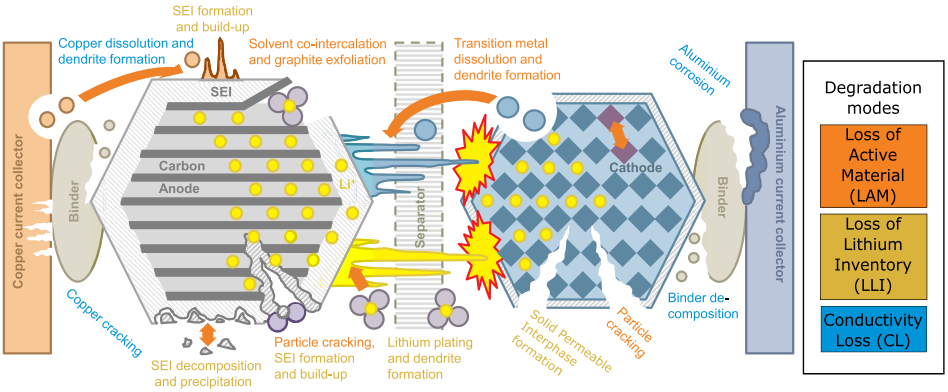

Fig. 1. Graphical illustration of the DMs and ageing mechanisms in LIBs, adapted from Refs. [11,30,32].

rate≤C/10) over the whole SoC window [3]. The pOCV curve plots the terminal voltage against the charge or SoC. Differentiating the pOCV curve with respect to the charge yields the DV curve (the IC curve is the reciprocal of the voltage derivative with respect to the charge) [3]. DTV is another thermodynamic technique which requires the measurement of the temperature and voltage when the battery is charged or discharged at C-rates ≤2C [17–19]. As a kinetic-based technique, EIS galvanostatic measurements are derived by applying a sinusoidal current and measuring the corresponding sinusoidal voltage [2]. The impedance is then calculated as the quotient of the complex voltage and the current. Schindler et al. [20] proposed the combination of a thermodynamic and kinetic model which requires the pOCV (thermodynamic based model) and EIS (kinetic based model) curves. Fig. 2 also shows that each diagnostic method is used to quantify DMs, which is the parameter considered by the BMS.

3.1. Pseudo-OCV

The pOCV based methods identify and quantify DMs based on the changes of pristine half-cell (HC) pOCV curves. These HC pOCV measurements are performed only once at laboratory conditions for a particular cell model. Measuring one sample is enough, and then this method can be applied repeatedly [11,12]. This feature makes it possible to consider this method as non-invasive. pOCV measurements emulates equilibrium conditions so that two or more phases with different lithium concentrations at the same chemical potential coexist. This enables us to infer changes in the electrochemical properties that physically can be measured through changes in charge, Q, and pOCV. An approximate equilibrium state is achieved if the cell is typically charged or discharged at very low currents (circa: ≤ C/25) whilst measuring Q and the pOCV [10]. Fig. 3 illustrates the general process of the pOCV based methods to quantify DMs.

The pOCV based methods operate in a backward basis, i.e. firstly the degradation is hypothesized and once this is proved, the hypothetical degradation is accepted as the true degradation. This process is divided into the following steps:

- **Step 1:** the expected DMs (LLI, LAM and CL) are hypothesized based on engineering rules (refer to Table 2) or use-life knowledge.
- **Step 2:** HC-pOCV measurements are performed once at laboratory conditions when the cell is new.
- **Step 3:** pristine HC-pOCV measurements are transformed into aged HC-pOCV measurements through simulation by using the hypothesized DMs from step 1.
- **Step 4:** the FC-pOCV at low C-rates (<C/25) is measured if the battery is charging (parking mode), or the FC-pOCV is estimated if the battery is discharging (driving mode).
- **Step 5:** the difference (error) between the simulated and the measured FC-pOCV is calculated.
- **Step 6:** the error obtained in step 5 is compared with a pre-defined threshold error (ε). The estimated error can be expressed as the absolute error or the Root Mean Square Error (RMSE). The value of ε is defined in an individual basis according to the requirements of each particular application. If this error is lower or equal than the pre-defined threshold, the hypothesized degradation is accepted. Otherwise, the hypothesized degradation is rejected. In this case, a new hypothesis is made and the whole process (steps 3 to 5) is repeated until the obtained error is lower or equal than ε. The value of ε is defined in an individual basis according to the requirements of each particular application. As an example, Marongiu et al. [12] obtains a maximum ε of 1.10% for the pOCV discharge and 0.98% for the pOCV charge process. A limitation of this method is that more than one hypothesis within the same iteration can be true and hence, the DMs may not be estimated uniquely. A solution for this would be to compare the result of the estimation with historical battery operating parameters (e.g., temperature, SoC, ΔDoD or C-rate). This would enable us to evaluate whether the hypothesized DMs are plausible with respect to the theory of battery degradation (refer to Table 2).

Though pOCV based methods follow the process depicted in Fig. 4, this review has categorised the pOCV based methods into 3 different groups. The main difference among the groups is the parameter used to relate the DMs with the shifts of HC-pOCV.

- **Group 1:** includes studies in which the relationship between HC-pOCV curves and DMs are determined according to the change of the charge-throughput and capacity ratio. The charge-throughput represents an indication of the amount of accumulated current (absolute value) that is stored (charging) and released (discharging) in the battery over time [2]. The capacity ratio is calculated as the ratio between the capacity of the NE with respect to the capacity of the PE. This method was initially proposed by Dubarry et al. [10] and further applied in Refs. [11,12,20].
- **Group 2:** includes studies in which the relationship between HC-pOCV curves and DMs is determined according to the change in SoC. SoC and capacity ratio (Group 1) has the same physical meaning, only the notation is different. This notation was used by the research group from Tsinghua University (China) and therefore, the reviewed articles related to this group are classified separately. In particular, the SoC representation was suggested by Han et al. [15], extended by Ouyang et al. [16] and applied in Refs. [37–39].
- **Group 3:** includes studies in which the relationship between HC-pOCV curves and DMs is determined according to the change in SoC. In contrast to Group 2, the studies of Group 3 introduce two parameters, m (equivalent to LAM) and δ (equivalent to LLI), to quantify the DMs. This method was initially presented by Honkura et al. [14,40] and further applied in Refs. [41,42].

Table 2
Relationship of the battery ageing extrinsic factors with the affected component, ageing mechanism, potential ageing effects, most pertinent DM, mechanism type and most pertinent observed effects [5,30].

Extrinsic factor	Level	Affected component	Ageing mechanism	Most pertinent DM	Mechanism type	Most pertinent observed effects
T	High (> 35 °C)	NE - Anode (Active material).	SEI growth.	LLI	Gradual.	CF&PF
			Particle fracture (with cycling).	LAM	Overstress.	CF&PF
		PE - Cathode (Active Material).	SPI growth.	LLI	Gradual.	CF&PF
			Gas generation.	LAM	Overstress.	CF
			Particle fracture with cycling).	LAM	Overstress.	CF&PF
		Current collectors.	Binder decomposition.	CL	Gradual.	PF
		Separator.	Closing of separator pores.	LAM	Overstress.	CF&PF
		Electrolyte (salts).	Decrease in lithium salt concentration.	LAM	Gradual.	PF
		Electrolyte (organic solvents).	Gas generation.	LAM	Overstress.	PF
T	Low (< 5 °C)	NE - Anode (Active Material).	Lithium plating and dendrite growth on anode surface.	LLI	Gradual.	CF&PF
C-rate	High (> 2C)	NE - Anode (Active Material).	Lithium plating and dendrite growth on anode surface.	LLI	Gradual.	CF&PF
			Particle fracture (with cycling).	LAM	Overstress.	CF&PF
			SEI growth.	LLI	Gradual.	CF&PF
		PE - Anode (Active Material).	Particle fracture (with cycling).	LAM	Overstress.	CF&PF
SoC	High (> 95%)	NE - Anode (Active material).	SEI growth.	LLI	Gradual.	CF&PF
			Particle fracture (with cycling).	LAM	Overstress.	CF&PF
		PE - Cathode (Active Material).	Gas generation.	LAM	Overstress.	CF.
		Current collector (PE-Cathode).	Pitting corrosion of aluminum.	CL	Gradual.	PF
		Current collectors.	Binder decomposition.	CL	Gradual.	PF
		Electrolyte (organic solvents).	Gas generation.	LAM	Overstress.	PF
SoC	Low (< 5%)	PE - Cathode (Active Material), mostly in LCO and LMO.	Reduction of sites.	LAM	Gradual.	CF&PF
		Current collector (NE-Anode).	Free copper particles of copper plating.	CL	Gradual.	CF&PF
ΔDoD	Large (> 80%)	NE - Anode and PE - Cathode (both active material).	Particle fracture.	LAM	Overstress.	CF&PF
			Reduction of sites.	LAM	Gradual.	CF&PF
Cycle number	Continuous	NE - Anode and PE - Cathode (both active material).	Particle fracture.	LAM	Overstress.	CF&PF
			Reduction of sites.	LAM	Gradual.	CF&PF

Fig. 4 provides an overview of the principle, required measurements, computation and output for each pOCV group.

Aside the mentioned differences, Table 3 summarises other differences among the groups. The characteristics which are not included in this table can be assumed the same for each Group.

3.2. Incremental Capacity - Differential Voltage (IC-DV)

A subset of the methods reviewed in Section 3.1 use IC and DV curves to identify DMs and thus, to corroborate the DMs quantified using HC-pOCV measurements. IC-DV curves are derived by

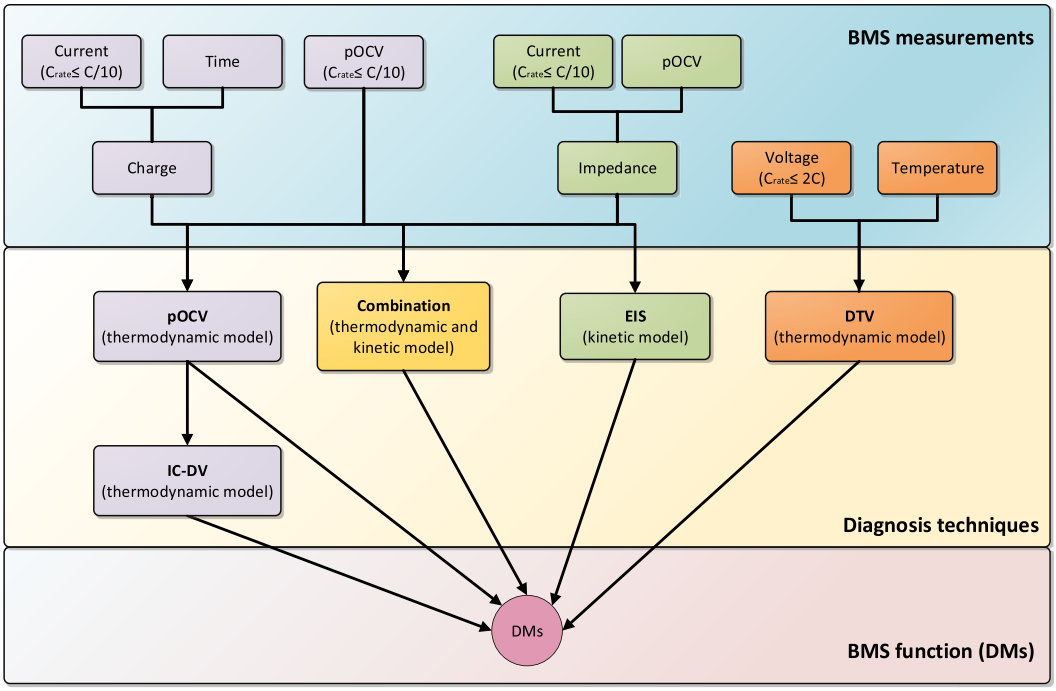

Fig. 2. Relationship between BMS measurements and DMs diagnosis techniques reviewed in this study.

differentiating the charge with respect to the pOCV (IC - dV/dQ), and vice versa, differentiating the pOCV with respect to the charge (DV - dV/dQ). As reported in Ref. [3], DMs can be quantified by observing changes in the IC-DV curves through ageing. According to the different possibilities to identify and quantify DMs by means of IC and DV curves, the IC-DV methods are classified into 3 groups.

- **Group 1:** includes studies which uses the IC-DV curves derived from

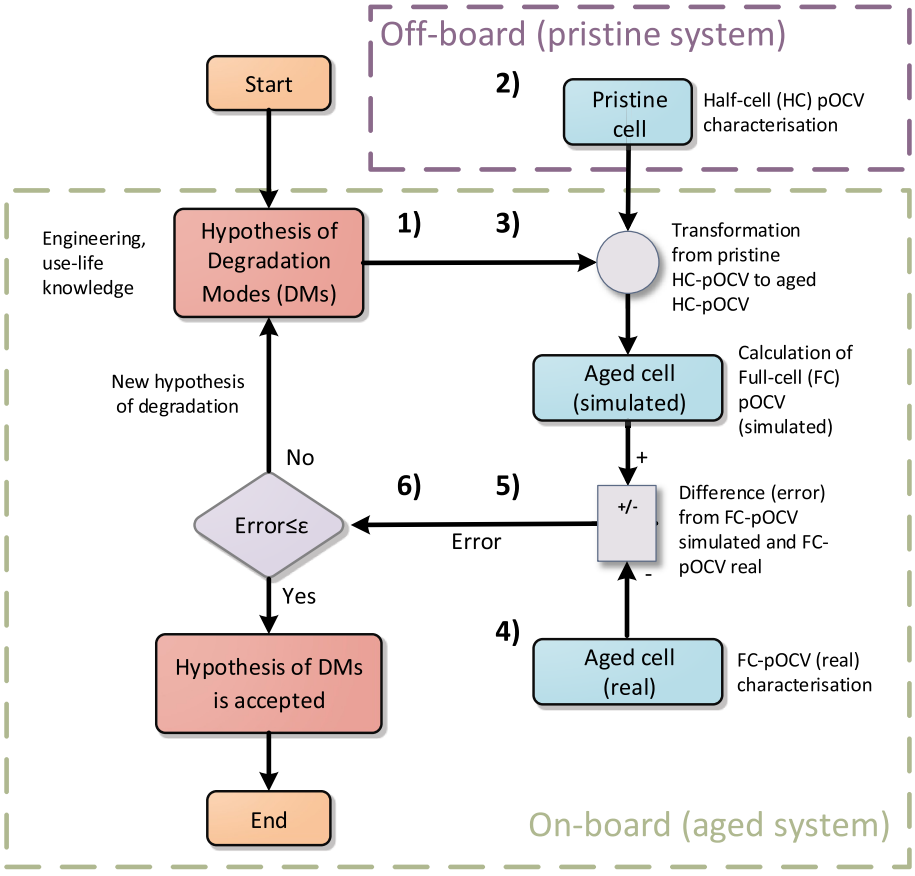

Fig. 3. Generic framework of pOCV based methods.

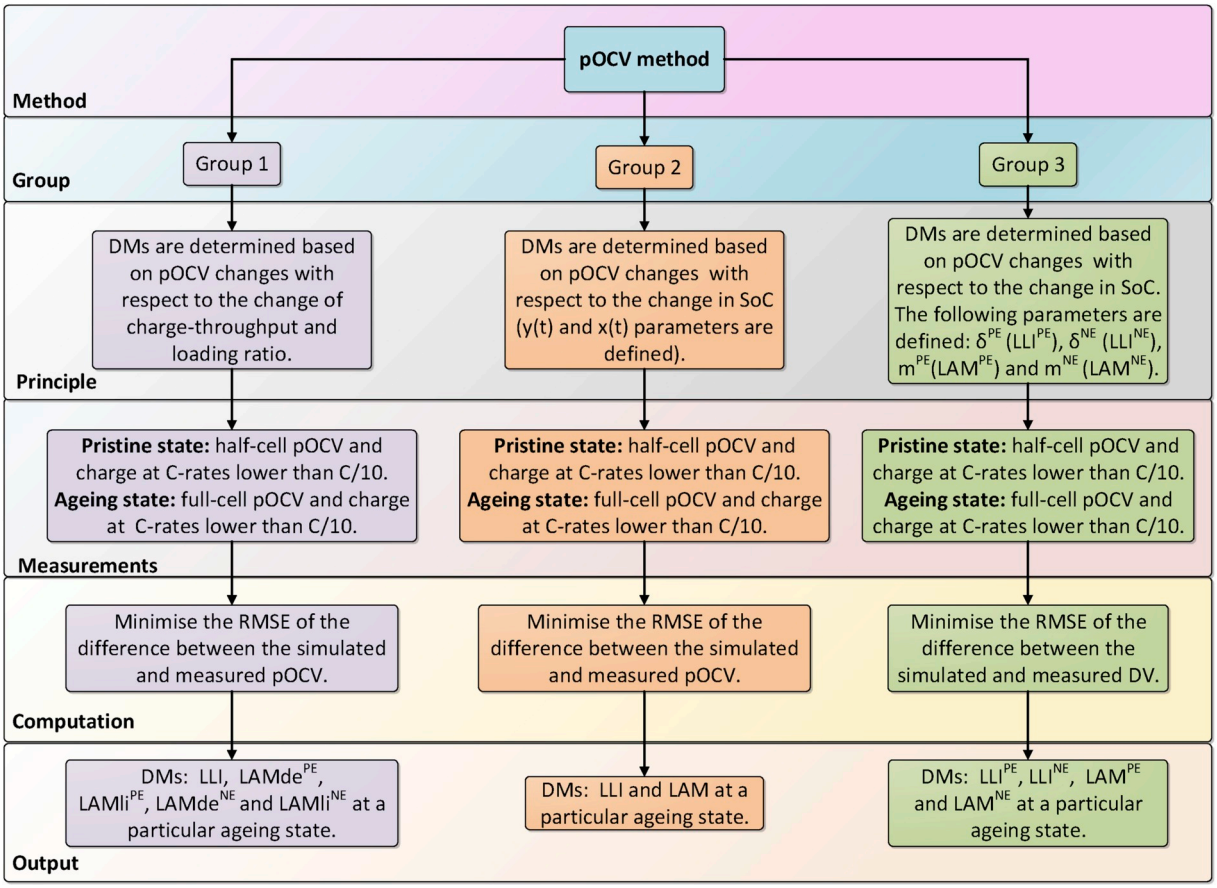

Fig. 4. Principle, required measurements, computation and output of each group of the pOCV technique.

the Group 1 pOCV methods. This approach was introduced by Dubarry et al. [10] and further applied in Refs. [43,44]. There are other studies [15,16,38,39,45–47] in which DMs are identified by making assumptions. As these studies do not follow an automated process, they are beyond the scope of this review.

- **Group 2:** constitutes the studies which relate the change of the Peak Area (PA) of the IC curves with DMs. This approach was firstly presented in Dubarry et al. [48] as an extension of the method initially presented in Ref. [10]. The PA can also be used to validate the DMs obtained from Ref. [10]. This approach has been developed by the researchers of Dubarry's research group [4,48,49] and [50].
- **Group 3:** comprises the studies which quantifies the DMs based on the change of particular points of the IC and DV curves. IC and DV curves are in this case derived based on full-cell measurements. Only two studies [3,51] were identified in this group.

Fig. 5 provides an overview of the principles, required measurements, computation and output for each IC-DV group. The DMs in Group 1 and 2 are derived using the same steps as in pOCV based techniques (refer to Fig. 3) with an additional step. This step calculates the IC and DV curves from the simulated pOCV curves once the hypothesized DMs are accepted. Then either the changes of the IC-DV curves (Group 1) or the changes of the PA of the IC curves (Group 2) are related to the changes in DMs. Instead of using HC-pOCV measurements as in Groups 1 and 2, the articles of Group 3 employ FC-pOCV measurements to directly quantify DMs based on the change of the IC-DV curves.

To maintain consistency with respect to the previous section,

Table 3
Differences among the characteristics of pOCV - Group 1, Group 2 and Group 3.

Characteristic	Group 1	Group 2	Group 3
Definition of DMs	LLI, LAM_{de}^{PE}, LAM_{li}^{PE}, LAM_{de}^{NE} and LAM_{li}^{NE}	LLI, LAM and R	LLI^{PE}, LLI^{NE}, LAM^{PE} and LAM^{NE}
Parameters used to relate DMs	LLI, LAM_{de}^{PE}, LAM_{li}^{PE}, LAM_{de}^{NE} and LAM_{li}^{NE}	x_0 and y_0	δ^{PE} (LLI^{PE}), δ^{NE} (LLI^{NE}) m^{PE} (LAM^{PE}) and m^{NE} (LAM^{NE})
Measurement of the resistance	No	Yes	No
Kinetics effects (e.g temperature)	No	Yes (in Ref. [16])	No
Method used to determine DMs	Difference between $pOCV_{sim}^{FC}$ and $pOCV_{meas}^{FC}$	Difference between $pOCV_{sim}^{FC}$ and $pOCV_{meas}^{FC}$	Difference between $dpOCV_{sim}^{FC}/dQ_{sim}^{FC}$ and $dpOCV_{meas}^{FC}/dQ_{meas}^{FC}$

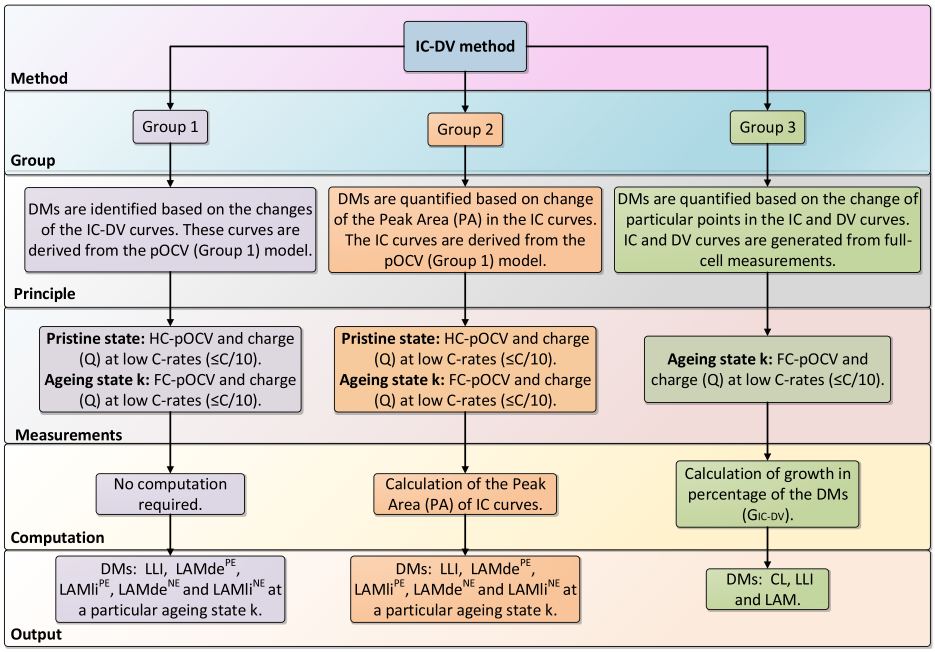

Fig. 5. Principle, required measurements, computation and output of each group of the IC-DV technique.

Table 4 summarises the main differences among the Group 1, Group 2 and Group 3 methods. The characteristics which are not included in this table are, again, assumed to be the same for each Group.

3.2.1. Group 1

The models of Group 1 correlates changes in IC and DV curves with the DMs. These DMs are previously identified using the pOCV Group 1 model [10]. Following on from electrochemistry principles, changes in IC and DV curves can be related to pre-determined DMs. For a LFP cell, Dubarry et al. [10] showed that the change of the height of the peaks of the IC curves at approximately constant voltage is related to LAM. Similarly, the shift of the DV curves to lower capacities is linked to LAM. For both cases, the pOCV changes slightly, and so implies the system is close to equilibrium and therefore the total overpotential is approximately zero. From an electrochemical viewpoint this scenario involves the movement of a low amount of Li-ions and therefore, these phase changes are mostly attributed to structure disordering of the active materials (LAM) [10,52]. The decrease of the height of the peaks and shift toward higher (charging) or lower (discharging) voltages of the IC curves is related to LLI. Likewise, the shift of DV curves toward lower capacities without shift of the DV peaks is associated to LLI. A reduction in the number of charge-transfer Li-ion intercalation and de-intercalation reactions leads to a decrease of the pOCV (IC) and the capacity (DV). Electrochemically these effects are mainly linked to LLI. It is noteworthy that it is difficult to distinguish between $LAMli^{PE}$ and LLI using the DV analysis. However, these DMs are clearly differentiated using the IC analysis. Hence, despite the fact that IC and DV curves are determined from the Q and pOCV relationship, both curves offer different insights into the rate and nature of the degradation within the cell.

Dubarry et al. [10] illustrates that a constant shift of the IC curves toward lower voltages is related to CL. Likewise, the authors show that a lack of change of the DV curves is connected to CL. Assuming a simple model representation of the battery to Ohm's law, the $pOCV$ is derived as the difference between the pure OCV, OCV, and the voltage drop due to the ohmic resistance, V_{ohm}.

$$pOCV = OCV - V_{ohm} = OCV - I \cdot R_{ohm} \quad (1)$$

Given a constant current flow and a constant OCV as it is the case, an increase in R_{ohm} will cause a decrease in $pOCV$. The increase in R_{ohm} is related to CL [53], which means that this only affects the cell voltage, not the capacity [10]. Therefore, without capacity fade, the effect of CL can be seen as a change in cell voltage [10].

3.2.2. Group 2

The authors in Refs. [4,48,49] relate the change of the PA of the IC curves with the DMs. This Group follows the same procedure as Group 1 (IC-DV) with the difference that the PA is calculated. The PA is calculated as subtracting the cell capacity at the voltage inflection points minus the cell end of discharge capacity. The capacity distribution is often given in terms of percentage of the total cell capacity. Computing the PA of the same peaks at different time instants (i.e. characterisation

Table 4
Differences among the characteristics of IC-DV - Group 1, Group 2 and Group 3*. *In contrast to Table 3, measurement of the resistance and kinetics effects are not considered for any of these methods. Thus, resistance measurements are not included here.

Characteristic	Group 1	Group 2	Group 3
Definition of DMs	LLI, $LAMde^{PE}$, $LAMli^{PE}$ $LAMde^{NE}$ and $LAMli^{NE}$	LLI, $LAMde^{PE}$, $LAMli^{PE}$, $LAMde^{NE}$ and $LAMli^{NE}$	LLI, LAM and CL
Parameters used to relate DMs	Changes in IC and DV curves	Peaks of IC curves	Changes in IC and DV curves
Method used to determine DMs	DMs are not quantified	Calculation of integral area determined by the inflection points of the IC peaks	Differences between $max(pOCV^{FC})$, $max(Q^{FC})$ and $max(\Delta Q^{FC}/\Delta pOCV^{FC})$

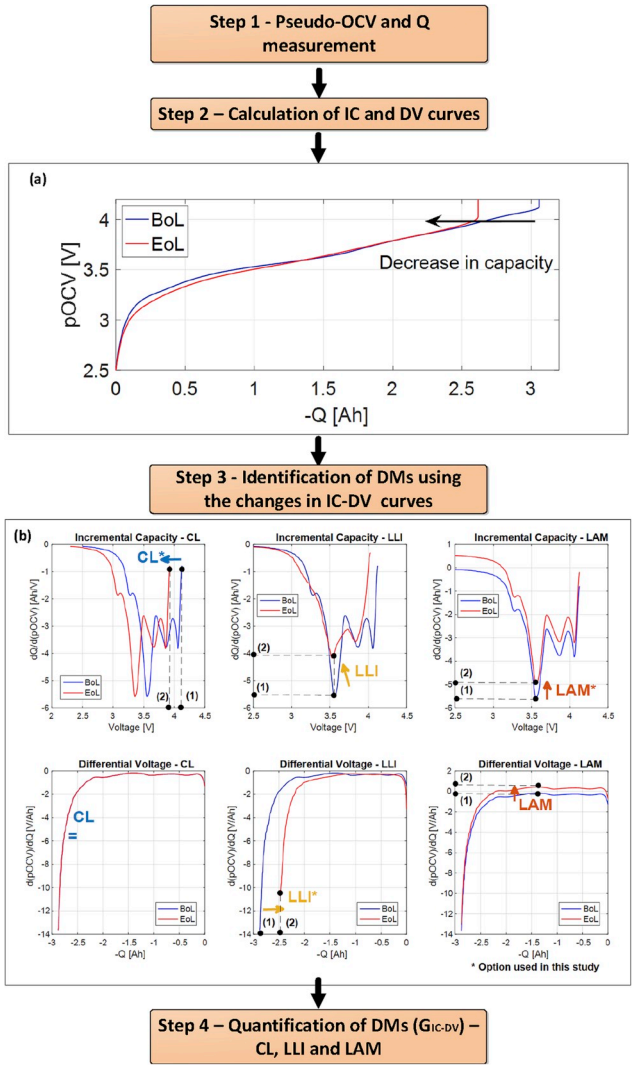

Fig. 6. Framework of the methodology employed in Refs. [3,51]. (a) FC pOCV measurement for BoL and EoL cell and (b) relationship of changes in IC and DV curves with the DMs.

tests) allows to observe the most pertinent DMs over ageing. This technique has the limitation that CL cannot be inferred.

3.2.3. Group 3

Pastor-Fernández et al. [3] quantify the DMs based on the changes of the IC and DV curves calculated from full-cell pOCV and charge measurements. Fig. 6 shows the framework of the methodology employed, which is composed by four steps.

- **Step 1:** consists of measuring the FC pOCV and charge (Q) at low C-rate (C/10).
- **Step 2:** the FC pOCV and Q measurements from step 1 are differentiated. From this, the IC and DV curves are derived.
- **Step 3:** following on from the conclusions from Ref. [10], the changes in IC and DV curves are related with the DMs in a generic way. Table 5 shows this relationship. As Dubarry et al. [10] study a LFP cell, this generic relationship may not be always true for other cell chemistries.

3.3. Electrochemical Impedance Spectroscopy (EIS)

EIS is a technique widely employed to measure the cell impedance along a range of frequencies, typically from mHz to kHz [3]. The majority of the studies identified in the literature [29,54–62] use EIS as a characterisation technique to infer ageing mechanisms without following an automated approach. In addition, some authors [63–65] study the on-board implementation of EIS through novel power electronic such as switched-inductor ladder topology, and control, such as digital proportional integral systems. It is seen that only the method from Pastor-Fernández et al. [3,66] relate specifically the changes of the EIS resistances with the DMs. Fig. 7 illustrates the steps to quantify DMs according to Refs. [3,66].

- **Step 1:** it consists of measuring the FC impedance using the EIS test.
- **Step 2:** the measured EIS spectrum from step 1 is fitted in step 2 using the non-linear least squares algorithm and the corresponding Adapted Randles-Equivalent Circuit Model (AR-ECM) is derived.
- Step **3:** it is known that one AR-ECM resistance comprises the change of more than a single DM, and theoretically it is not possible to isolate the causality between a single ageing mechanism, DM and electrical component within an ECM representation. Despite this, Step 3 proposes a relationship between each resistance of the AR-ECM and the most pertinent DMs as shown Table 6. This relationship is a first step to link each resistance of the AR-ECM with individual effects of DMs. For instance, other studies such as [20] proposed an alternative procedure to relate the EIS resistances with the DMs. Therefore, there is no unique way to relate AR-ECM resistances with the effects of DMs, and thus, further work is required in this respect.

3.4. Combination of thermodynamic (pOCV) and kinetic (EIS) methods

Schindler et al. [20] proposed an automated model to couple two battery dynamic concepts: thermodynamics (HC- and FC-pOCV measurements) and kinetics (internal resistance). The structure of this model is composed by two sub-models: a pOCV model to quantify LAM and LLI, and an EIS based model to quantify the overpotential due to Li-ion kinetics. The steps of the pOCV model are the same as in pOCV Group 1 method with two main differences. Firstly, the transformation of pristine HC-pOCV into aged HC-pOCV measurements (refer to step 3 in Fig. 3) considers a gradual change of the NE pOCV (shrinkage) rather than a constant change. Schindler et al. [20] established this gradual change because the active material loss across the SoC window is not uniform. Secondly, following on from the studies of pOCV Group 3 [14,40–42], Schindler et al. [20] use a RMSE cost function based on DV curves to determine the DMs. The DV data is better amplified than the pOCV data, and hence, solving the RMSE cost function using DV data leads to a more reliable result than using pOCV data. Although EIS measurements are considered in this method, CL is not quantified. The EIS based model is employed to consider the amount of LLI and LAM overpotential (pOCV) due to kinetic effects [20]. For this, the voltage drop due to R_{ohm} is related to the overpotential (pOCV) caused by LLI and the voltage drop due to R_{pol} ($R_{ohm}+R_{ct}$) is related to the overpotential (pOCV) caused by LAM [20]. Fig. 8 illustrates the steps to quantify DMs based on the Schindler et al. [20] model.

3.5. Differential Thermal Voltammetry (DTV)

Initial studies of Reyner et al. [67] and Maher et al. [68] demonstrated that changes in the entropy profiles can be used as an indication of the ageing mechanisms occurring in either the PE or NE. Later, Wu et al. [17], Merla et al. [18,19] and Offer et al. [69] proposed the DTV technique to obtain information of the entropic behaviour of the cell by taking the temperature profile of the cell surface during galvanostatic charge/discharge. These authors [17–19] infer ageing mechanisms by applying the DTV technique, but they do not show the capability to identify and quantify DMs. Fig. 9 illustrates the steps to infer DMs based on the DTV technique. Thus, following the systematic approach specified by the criteria from Section 5.1, this technique could be excluded

Table 5
Relationship between the changes in IC and DV curves with the most pertinent DM [3].

- **Step 4:** the growth in percentage is defined to quantify each DM. This parameter is computed as the difference (in percentage) between the current ageing state k and the initial ageing state of the maximum pOCV value for CL, the maximum dQ/dV value for LAM and the maximum Q value for LLI.

Change in IC curve	Unit	Change in DV curve	Unit	DM
Decrease of the height of the peaks at approximately constant voltage.	[Ah V^{-1}]	Shift of the DV curves to lower capacities.	[V Ah^{-1}]	LAM
Decrease of the height of the peaks and shift toward higher voltages.	[Ah V^{-1}] and [V]	Shift of DV curves toward lower capacities without shift of the DV peaks.	[Ah]	LLI
Shift toward lower voltages.	[V]	Lack of change	[Ah]	CL

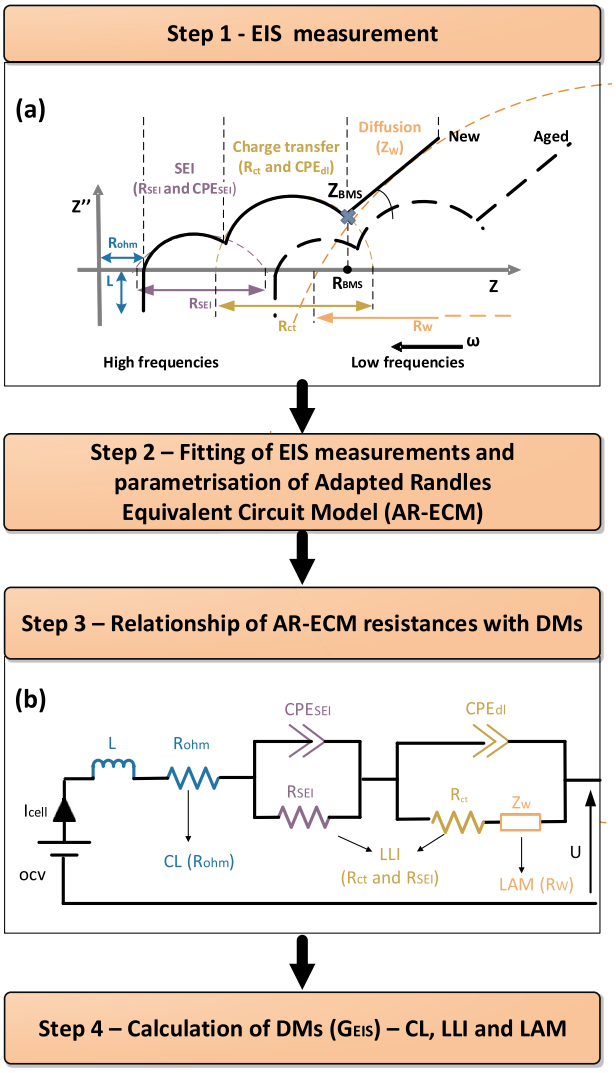

Fig. 7. Framework of the methodology employed in Refs. [3,66]. (a) Relationship of EIS spectrum with kinetic Li-ion battery processes and (b) relationship of AR-ECM components with DMs.

from this review because their corresponding studies neither identify nor quantify DMs. However, the ageing mechanisms are directly related to the DMs and for completeness, this technique has been considered as a part of this review.

4. Requirements on battery monitoring algorithms

In the process of designing a diagnostic function, it is needed to ensure that a minimum amount of requirements are fulfilled. The articles are then reviewed according to the requirements characteristic of automotive applications. This review would ultimately support the implementation of these techniques in real-world applications. It is noteworthy that this list is not exhaustive and more requirements can be added based on the particularities of each system design.

Table 6
Relationship between the resistances of the AR-ECM with the most pertinent DM.

- **Step 4:** the growth in percentage is defined to quantify each DM. This parameter is computed as the difference (in percentage) between the current ageing state k and the initial ageing state of the R_{ohm} value for CL, the R_{SEI} plus R_{ct} values for LLI and the R_W value for LLI.

AR-ECM component	Unit	Most pertinent DM
Increase in R_{ohm}	[Ω]	CL
Increase in R_{SEI} & R_{ct}	[Ω]	LLI
Increase in R_W	[Ω]	LAM

- **Universality:** according to automotive standards such as MISRA [70], there is a need to adapt diagnostic algorithms to the different cell technologies without modifying the algorithms significantly.
- **Real application capability:** the framework defined for the methods reviewed should be simple enough to be implemented in real applications, e.g., within a BMS. In general, a diagnostic method is simple enough when it has the potential to fulfill commercially viable software and hardware requirements [21,24]. Hardware and software requirements are defined below.
  - **Hardware (HW) requirements:** the DM diagnostic algorithm needs to consider the characteristics of the target hardware where the diagnostic algorithm is executed. Following on from Ungurean et al. [24], HW requirements are divided into data processing mode and processing time. Data processing mode denotes how the DMs are being quantified. This process can be done offline and online (refer to Section 1). Processing time is related to the time needed by the diagnostic algorithm to produce the estimation of the DMs. This time depends mainly on the complexity of the method and the power of the MCU used.
  - **Software (SW) requirements:** the DM diagnostic method needs to consider also the requirements of the target software where the diagnostic algorithm is programmed [21,24]. According to Ref. [71], these requirements include functionality, reliability, usability, efficiency, maintainability, portability and traceability. It is beyond the scope of this study to discuss each of these requirements in detail; they are however described fully in a number of standards and guidelines such as ISO 9126 [71] and MISRA [70,72].
- **Consideration of real-world conditions:** diagnostic models need to be validated under scenarios close to real-world conditions. An example would be to degrade cells with non-repetitive real driving cycle data where ageing factors change randomly [28].
- **Accuracy and precision:** since LIBs are non-linear and time-variable systems, estimating the DMs with a low level of uncertainty is a challenge [1,21,24]. The level of uncertainty is measured with two parameters: accuracy and precision. Within the context of

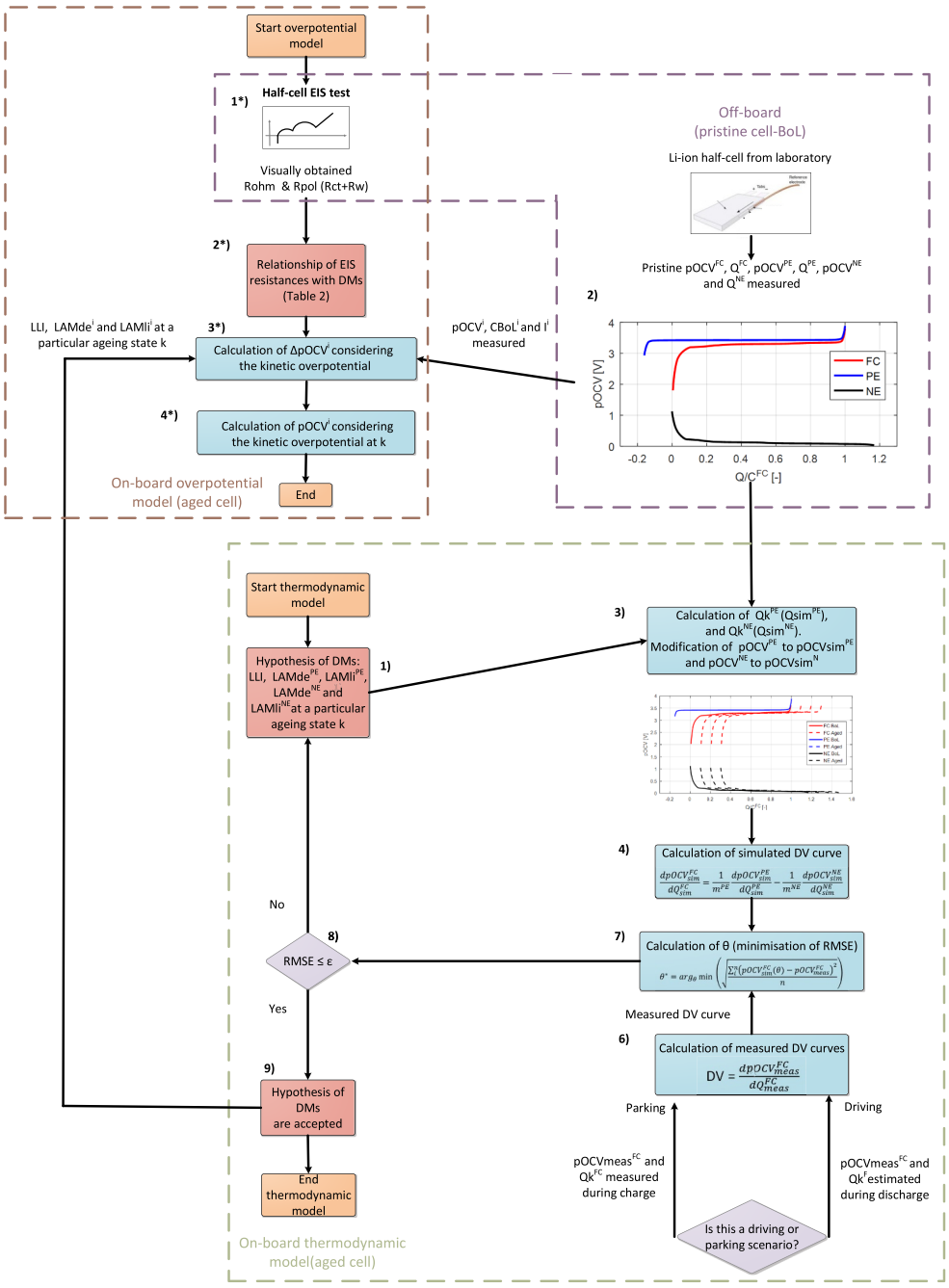

Fig. 8. Framework of Schindler et al. [20] model.

quantification of DMs, accuracy and precision levels are difficult to calculate. This complexity arises because the true value of this metric cannot be easily derived, even if more complex electrochemical techniques such as SEM or XPS are used. Thus, accuracy and precision are determined indirectly by calculating the error of the parameter used to quantify the DMs. For instance, Marongiu et al. [12] use the difference in pOCV to approximate accuracy.

- **Robustness:** the reviewed methods should ensure optimal performance for different operating conditions [21,24]. This means a method needs to be tested with a different type of input data (e.g., time-varying ambient temperature, current, SoC and ΔDoD) considering typical scenarios of vehicle operation (e.g., driving or parking). Depending on the scenario the ageing effects could be different. For instance, long periods of parking resulting in battery self-discharge (low SoCs) may lead to particular DMs (e.g., copper plating on the negative current collector) [5] which are not common during driving operation (refer to Table 2).
- **Scalability from cell to module and battery pack:** although the majority of methods are developed for cell level, they should be scalable to module and pack level in view of a potential real application [73].

5. Systematic and critical review of methods to identify and quantify DMs

As in Ref. [24], this review follows a systematic method. According to Tranfield et al. [74], systematic reviews differ from traditional narrative reviews by adopting a replicable, scientific and transparent

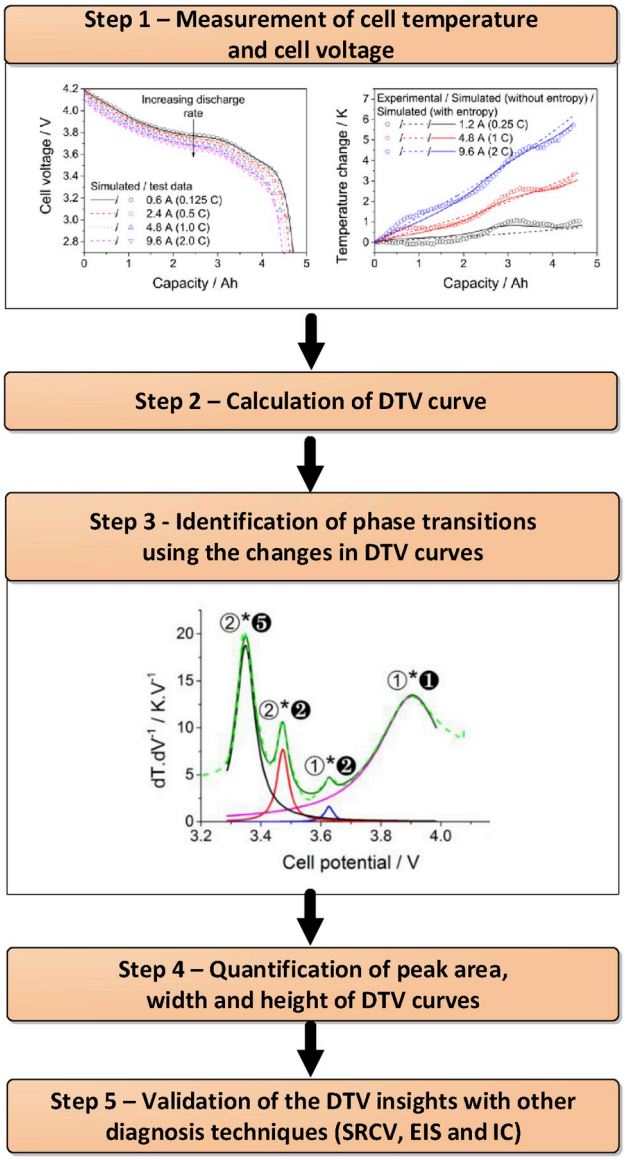

Fig. 9. Framework of Li-ion diagnosis by means of DTV curves.

process that aims to minimise bias through exhaustive literature searches of published and unpublished studies. The main limitation of systematic reviews is the lack of flexibility. For instance, following a consistent analysis could lead to the loss of important information which is not seen within the specified review criterion [75]. Other related problems are the inappropriate subgroup analysis to fulfill the review criterion, or the conflict with new experimental data which cannot be categorised within the review criterion [75]. These problems were mitigated in this work by considering some flexibility in the criterion used. The level of flexibility was argued in each case. An example of this is given in Section 5.7 for the DTV technique. The DTV technique related studies neither identifies nor quantifies directly the DMs. Further information concerning the steps to conduct a systematic review can be found in Ref. [75].

5.1. Evaluation criterion

For this study, 14 metrics were initially used to review the method described in each article systematically as shown Table 7. The first three metrics (automated, identification and quantification) are intrinsically related to the type of techniques evaluated in this study. The rest of the metrics (4) to (14) are derived from the requirements described in Section 4. Additionally, the next metrics were included as a part of the review to have a better understanding of the research groups involved in the field and the impact of their publications:

- Main author of the article.
- Research group.
- Country of the research group.
- Month (if available) and year when the article was online.
- Conference proceedings or journal in which the article was published.
- Number of citations of each article according to Google Scholar records [76]. The number of citations was recorded on 8th July 2018.

Following on from this criterion, tables are included to review the articles systematically in Section 5.2, Section 5.3, Section 5.5 and Section 5.7 for pOCV, IC-DV, EIS and DTV technique, respectively. The contributions and drawbacks of each article are highlighted. It is beyond the scope of this study to describe the particularities of each article reviewed. For this, it is recommended to refer to the corresponding citations.

5.2. Pseudo-OCV

5.2.1. Group 1

Table 8 evaluates the articles of Group 1 according to the criteria specified in Section 5.1. The model proposed by Dubarry et al. [10] in 2012 is quite complete because apart from quantifying LLI, LAM and CL, it also determines two other DMs: faradic rate degradation and formation of parasitic phase. From the same research group of Dubarry or through collaborations, their model was further applied in different scenarios in Refs. [4,43,44,48,49]. Since these studies emphasize the use of IC and DV techniques to identify [43,44] or quantify [4,48,49] the DMs, their review was included in Section 5.3.1 and Section 5.3.2, respectively. The main contribution of this study is to analyse the impact of different types of DMs on different LIB aspects as described above. The main drawback of the approach presented by Dubarry et al. [10] is the lack of evidence to implement it on-board. This problem is faced in the model presented by Marongiu et al. [12]. The authors adapted the model proposed by Dubarry et al. [10] to quantify DMs on-board of a.

LFP cell cycled by a repetitive dynamic profile at room temperature (25 °C). This model is composed by an offline and online part as described in Fig. 3. This study stands out with respect to the literature because of the capability to quantify DMs on-board using input data from different scenarios (parking and driving). Although this method was tested for LFP cells, it can also be applied to other cell chemistries similarly as the method proposed by Dubarry et al. [10]. As pointed out in Section 3.1, the main drawback of this approach, that has not resolved up to date, is that the DMs may not be estimated uniquely as more than one hypothesis of DMs within the same iteration may be true.

Following on from Ref. [10], Birkl et al. [11] also proposed a parametric model to identify and quantify LLI and LAM by estimating the shifts of HC and FC-pOCV curves. The contribution of this study is the derivation of the DMs as a manifestation of a host of different physical and chemical mechanisms. However, previous studies [10,12,43,49] determined the DMs using a less detailed electrochemical formulation making these models more suitable for BMS on-board applications.

Based on Dubarry's et al. model [10], Ma et al. [77] apply particle swarm optimisation algorithm (PSO) to parametrise the half-cell model considering the individual electrode behaviour and battery OCV at different ageing levels. Following this model, the corresponding DMs are quantified and the conclusions agree with the results obtained via

Table 7
Metrics used to conduct the literature review.

Metric	Description
(1) Automated	An article is related to Y (Yes) if the diagnostic method is automated; or to N (No), if not. A diagnostic method is automated if follows a step-by-step process to identify or/and quantify the DMs. Automated processes are desired for further hardware and software implementation of a diagnostic technique [24].
(2) Identification	An article is related to Y if the diagnostic method identifies the DMs; or to N, if not.
(3) Quantification	An article is related to Y if the diagnostic method quantifies the DMs; or to N, if not.
(4) Universality	An article is related to Y if the diagnostic method is universal; or to N, if not.
(5) On-board capability	An article is related to Y if the method can be implemented on-board; or to N, if not.
(6) Method	Describes the method or group of methods used (pOCV, IC-DV, EIS or DTV) in an article.
(7) Cell chemistry type	Describes the cell chemistry type or types to which the method was applied (e.g., NCA, NMC, LFP, etc …).
(8) Input data form	Input data form can be repetitive real drive cycles (RDC), repetitive synthetic (artificial) cycles (RS), or calendar (CAL).
(9) Data processing mode	Denotes when the acquired battery parameters are being processed: offline (Off) and online (On).
(10) Processing time	An article is related to S if the time needed to produce the first estimation is short (S < 30min); or to M if it is mid (30min≤M≤60min); or to L if it is long (L > 60min); or to n.a. if the processing time is not available. As none of the reviewed studies attempt to implement the diagnostic methods into a real-time hardware environment, the reported processing time is related to e.g., MATLAB software simulations.
(11) Accuracy level	Provides the degree to which the result obtained by applying the method is closer to the true result. The accuracy in the determination of the DMs cannot be directly calculated as explained in Section 4. This calculation is determined indirectly by calculating the error of the estimation of the pOCV or capacity (C). Different metrics such as the absolute error or the RMSE are used to express the estimation error. In case the accuracy level is not indicated, then the accuracy level of a particular diagnostic approach is related to NEV (not evaluated).
(12) Robustness	A method is robust if given different data as input the accuracy of the estimation result keeps at the same level. Each article is related to Y if the method is robust; or to N if not; or to NEV if robustness is not evaluated.
(13) Scalability	An article is related to Y if the method is scalable from cell to module and pack; or to N if not; or to NEV if scalability is not evaluated.
(14) HW implementation	An article is related to Y if the HW implementation of the method is studied; or to NEV if not. Note that the studies reviewed do not consider software requirements and thus, this metric is not considered in this criterion.

IC and DV analyses. The main contribution of this study is to quantify DMs applying the PSO algorithm. The main limitation of this study is the lack of guidelines to implement this methodology in real-world scenarios.

5.2.2. Group 2

Table 9 evaluates the articles of Group 2 according to the criteria specified in Section 5.1.

An alternative to the method proposed by Dubarry et al. [10], Han et al. [15] presented an approach to quantify DMs using the shifts of HC- and FC-pOCV curves. Similarly to Ref. [10], IC curves were calculated to identify the DMs in a qualitative manner. These qualitative insights corroborated the quantification of the DMs determined by pOCV curves. In addition, Han et al. [15] explain clearly the on-board capability of the IC curves using the point counting method. The simplicity and low computation requirements of this method make it suitable for BMS on-board applications. As a disadvantage, the point counting method may not be suitable to calculate the IC curves for the cases when the charging data is corrupted by noise. Further work includes testing this method using real BMS measurements, which often contain a large amount of noise.

Han's et al. degradation model was applied to quantify the DMs in different scenarios in Refs. [37–39] by authors of the same research group. Feng et al. [37] analysed the DMs of a 25 Ah NMC cell exposed to extreme temperatures (> 80 °C) without achieving thermal runaway. Ouyang et al. [38] evaluated the influence of the charging C-rate and the cut-off voltage limit on the DMs of 11.5 Ah LFP cells cycled at low temperature (−10 °C). Yan et al. [39] studied the DMs in four High Power (HP) Li-ion batteries cycled with a durability HEV profile at high temperatures (30 °C, 40°Cand 50 °C). For each of these cases, the quantification of the DMs using pOCV and Han's model IC curves were corroborated with the analysis of experimental IC curves. Ouyang et al. [16] extend the automated pOCV model presented by Han et al. [15] and further applied in Refs. [37–39]. Ouyang et al. [16] consider chemical kinetic principles in the calculation of $x(t)$, $y(t)$ and R. Apart from using a novel mathematical formulation, the main contribution of this study is that the degradation model was applied under realistic scenarios. These scenarios are a frequency regulation profile for storage grid applications and a dynamic BEV profile was used as inputs of the pOCV model to quantify the DMs. Additionally, DMs were also studied for a battery pack cell-to-cell variability scenario. Despite these contributions, the authors highlighted that a more detailed test matrix to

Table 8
Systematic and critical evaluation of the articles of Group 1 (pOCV) according to the criteria specified in Section 5.1. **(1–5) And (11–14) see Section 5.1 for the definition:** Y (Yes), N (No), NEV (Not Evaluated), NQ (Evaluated but Not Quantified) and n.a. (not available).
(8) Type of input data: C (Calendaric data), RS (Repetitive Synthetic data) and RDC (repetitive Real Drive Cycle data).
(9) Data processing mode: Off (Offline) and On (Online).
(10) Processing time: S (Short, S < 30min), M (Mid, 30min≤M≤60min), L (Long, L > 60min) and n.a. (not available).

Article	Main author	Research group	Country	Available online	Journal	# cits.	Evaluation criteria 1	2	3	4	5	6	7	8	9	10	11	12	13	14
[10]	Dubarry	HNEI	USA	Jul-12	JPS	206	Y	Y	Y	Y	NEV	pOCV &IC-DV	LFP	CAL	Off	n.a.	NEV	Y	NEV	NEV
[12]	Marongiu	RWTH	Germany	May-16	JPS	8	Y	Y	Y	Y	Y	pOCV	LFP	RDC	Off&On	n.a.	1.10% in C	Y for C_{test}	NEV	NEV
[11]	Birkl	Oxford	UK	Dec-16	JPS	46	Y	Y	Y	Y	N	pOCV	LCO& NCO	RS	Off&On	n.a.	< 3 mV pOCV	NEV	NEV	NEV
[77]	Ma	Univ. Beijing Institute	China	May-18	JPS	0	Y	Y	Y	Y	Y	pOCV&IC-DV	NMC	RS	Off	n.a.	& 8% DMs < 7 mV & RMSE pOCV	NEV	NEV	NEV

Table 9
Systematic and critical evaluation of the articles of Group 2 (pOCV) according to the criteria specified in Section 5.1. See definition of numeration (1) to (14) in Table 8.

Article	Main	Research	Country	Available	Journal	#	Evaluation criteria													
	author	group		online		cits.	1	2	3	4	5	6	7	8	9	10	11	12	13	14
[15]	Han	Tsinghua Univ.	China	Nov-13	JCP	187	Y	Y	Y	Y only IC	n.a.	pOCV &IC	LTO, LFP & LMO	RS	Off&On	S	< 5 mV (FC-pOCV)	NEV	NEV	NEV
[37]	Feng	Tsinghua Univ.	China	Sep-14	JPS	40	Y	Y	N	Y	NEV	pOCV &IC	NMC	RS	Off&On	n.a.	NEV	NEV	NEV	NEV
[38]	Ouyang	Tsinghua Univ.	China	Mar-15	JPS	53	Y	Y	Y	Y	NEV	pOCV &IC	LFP	RS	Off&On	n.a.	NEV	NEV	NEV	NEV
[16]	Ouyang	Tsinghua Univ.	China	Dec-15	AE	35	Y	Y	Y	Y	NEV	pOCV &IC	LFP, LMO + NMC	RS	Off&On	15min /1000 cycles	8% pOCV	Y	Y	NEV
[39]	Yan	Tsinghua Univ.	China	Jul-16	AE	9	Y	Y	Y	Y	NEV	pOCV &IC	LTO + NMC, LMO& SC	RDC	Off&On	15min /1000 cycles	8% pOCV	Y	Y	NEV
[46]	Lu	Harbin Institute of Technology	China	Feb-17	ECS	1	Y	Y	N	Y	N	pOCV &IC-DV	NMC	CAL	Off&On	n.a.	NEV	NEV	NEV	NEV

calibrate the model's parameters more precisely for different operating scenarios is needed.

From a different research group as [16,37–39], Lu et al. [46] adapted the automated model of Han et al. [15] to identify and quantify DMs. In addition to the automated model, they proposed a novel empirical expression for predicting LAM. The nonlinear least squares method was used in this case to solve the RMSE equation, and hence, quantify the parameters related to the DMs. The results revealed that the capacity fade during this calendaric investigation was predominantly caused by LLI and self-discharge. These results were qualitatively proven using IC and DV analysis. The main drawbacks identified for this model were: 1. lack in the capability to be applied on-board; 2. lack of robustness since the model was only validated for storage conditions and it may not be valid for other scenarios.

5.2.3. Group 3

Table 10 evaluates the articles of Group 3 according to the criteria specified in Section 5.1.

In 2008 Honkura et al. [14] published the first article ever found in which DMs are quantified following an automated model. As described in Section 3.1, Honkura et al. [14] quantified LAM and LLI tracking over time the changes in the amount of accessible active material, m^i, and the initial difference of Q^{PE} and Q^{NE} with respect to Q^{FC}, δ^i. Honkura et al. [40] published in 2011 a similar article where apart from quantifying the DMs as in Ref. [14], the authors also predict them using the $t^{1/2}$ rule. A year later, Dahn et al. [41] implemented this technique in a software package to quantify DMs in an automated way. None of these articles attempted to evaluate the on-board capability of the pOCV + DV method until 2016 with the publication of Hu et al. [42]. Hu et al. [42] compute m^i and δ^i in a two iteration process rather than deriving these parameters simultaneously. The advantage of the computation method suggested by Hu et al. [42] is that the electrode slippages, δ^{PE} and δ^{NE}, are easier to estimate by observing changes in the peaks of the DV curve than by comparing the estimated and measured DV data. However, the authors identified that the following issues remain to be addressed: 1. how to use FC-DV curves measured during a partial charge cycle to estimate the degradation parameters; 2. how to remove the noise in on-board measurements of FC pOCV and Q, and make the parameter estimation robust.

5.2.4. Benefits and limitations of pOCV groups

Analysing Table 8, the advantages and disadvantages of the method of each Group are compared in Table 11. In the case that not all the articles of a group fulfill a particular metric, the references of the articles that fulfill this are shown; or if none of the articles within a group fulfill a particular metric, then the cell is left blank. It is seen that the methods of Group 1 and 2 are the most feasible methods to quantify DMs on-board in commercial BMS applications because they fulfill most of the aspects defined in Section 5.1: (1–9) and (11–12) for Group 1; and (1–4), (6–13) for Group 2. In contrast, the articles of Group 3 only fulfill (1–6) and (9–10). The differences between the articles of Group 1 and 2 are: 1. the on-board capability and 2. the processing time and robustness of the method. Group 1 has a better on-board capability than Group 2. However, Group 2 fulfills processing time and robustness in comparison to Group 1. Despite Group 3 does not fulfill (7), (8), (11), (12), (13) and (14), the method is suitable for on-board applications as shown in Ref. [42]. The recommendation would be to choose a method of Group 1. To prove the robustness requirement, the chosen method would need to be validated with different input data forms.

5.3. Incremental Capacity - Differential Voltage (IC-DV)

5.3.1. Group 1

Table 12 evaluates the articles of Group 1 according to the criteria specified in Section 5.1.

Aside quantifying the DMs using HC-pOCV measurements as

Table 10
Systematic and critical evaluation of the articles of Group 3 (pOCV) according to the criteria specified in Section 5.1. See definition of numeration (1) to (14) in Table 8.

Article	Main author	Research group	Country	Available online	Journal	# cits.	Evaluation criteria 1	2	3	4	5	6	7	8	9	10	11	12	13	14
[14]	Honkura	Hitachi Ltd.	Japan	2008	ECS	30	Y	Y	Y	Y	N	pOCV&DV	NMC	C	Off&On	NEV	NEV	NEV	NEV	NEV
[40]	Honkura	Hitachi Ltd.	Japan	Aug-2011	JPS	56	Y	Y	Y	Y	N	pOCV&DV	NMC	CAL	Off&On	n.a.	20% C_{est}	NEV	NEV	NEV
[41]	H. Dahn	Dalhousie Uni.	Canada	Aug-2012	ECS	66	Y	N	N	Y	N	pOCV&DV	LCO	RS	Off&On	S	0.0001 V/mAh	NEV	NEV	NEV
[42]	Hu	Iowa State Uni.	USA	Aug-2016	ASME	0	Y	Y	Y	Y	Y	pOCV&DV	LCO	RS	Off&On	n.a.	NEV	N	NEV	NEV

Table 11
Comparison of the benefits and limitations of the methods of Group 1, 2 and 3 according to the evaluation criteria described in Section 5.1. See definition of numeration (1) to (14) in Table 8.

Group	Evaluation criteria 1	2	3	4	5	6	7	8	9	10	11	12	Key 13	14	articles
Group 1 [10–12]	✓ [All]	✓ [All]	✓ [All]	✓ [All]	✓ [12]	✓ [All]	✓ [11]	✓ [12]	✓ [All]	✗	✓ [11,12]	✓ [10]	✗	✗	[10,12]
Group 2 [15,16,37–39,46]	✓ [All]	✓ [All]	✓ [All]	✓ [15,16,37–39]	✗	✓ [All]	✓ [15,16,39]	✓ [39]	✓ [All]	✓ [15.16, 39]	✓ [16,39]	✓ [16,39]	✓	✗	[15,16]
Group 3 [14,40–42]	✓ [All]	✓ [14,40,42]	✓ [14,40,42]	✓ [41,42]	✓ [42]	✓ [All]	✗	✗	✓ [All]	✓ [41]	✗	✗	✗	✗	[42]

described in Section 5.2.1, Dubarry et al. [10] also introduces the theory to relate the changes of IC and DV curves with DMs. This theory can be used as a guideline to identify DMs in an automated way as suggested in Refs. [3,51]. Devie et al. [43] study the most pertinent DMs involved with and without overcharging a LTO and a NMC pouch cell. For the DMs that were initially hypothesized, IC-DV curves were used to identify DMs. Further work includes achieving a better understanding of the electrochemical processes that lead to the DMs. Since the same model and type of data was used as in Ref. [10], the contributions and drawbacks of this article are the same as in Ref. [10]. Berecibar et al. [44] used IC curves generated with the Dubarry et al. [10] model to highlight the differences in terms of DMs between NMC HP and NMC HE cells. The DMs were in this case identified by visual inspection of the changes in the IC curves without following any automated procedure.

Dubarry et al. [78] present an approach that can cover all the possible voltage curves upon degradation to fit the voltage response during constant current steps to decipher DMs. The voltage curves are derived from simulations using the model proposed in Ref. [10]. These curves are stored in the form of a look-up table that can be easily implemented in real-world applications. The authors also define feature of interests (FOI) from IC curves with the aim of relating the change of these FOIs with possible degradation paths. The main limitations of this approach are that chemistries with large voltage plateaus might be difficult to diagnose, the computation effort is high, and some FOIs could disappear with ageing providing an erroneous diagnosis.

5.3.2. Group 2

Table 13 evaluates the articles of Group 2 according to the criteria specified in Section 5.1.

Dubarry et al. [48] introduces the PA methodology in commercial HE and HP LFP cells. In deeper, Anseán et al. [49] use PA analysis of IC curves and Dubarry's et al. model [10] to identify and quantify the DMs for a standard charging event and a fast charging event (4C) of a HP LFP cell. Since the same model was used, the drawbacks of the PA analysis of IC curves for this study are the same as the ones described previously for [10]. Similarly, as in Ref. [49], Anseán et al. [4] quantify the reversible and irreversible part of lithium plating in commercial LFP cell cycled at constant temperature (23 °C).

Gao et al. [50] reveal the influence of different charging current rates and cut-off voltages on the aging mechanism of batteries by using PA IC analysis. In comparison to the rest of the studies of this group [4,48,49], Gao et al. [50] do not use Dubarry's et al. model [10] to quantify DMs based on the changes of HC-pOCV curves. Instead, the authors relate the changes of the IC peaks with DMs by visual inspection and then, the area of each peak is calculated. The main contribution of this study is that DMs were quantified based on PA IC analysis without using HC-pOCV measurements. The main limitation of this approach is the amount of subjectivity involved when DMs are detected through visual inspection. Further work includes developing an automated process to reduce the subjectivity in the interpretation of the IC peaks.

5.3.3. Group 3

Table 14 evaluates the articles of Group 3 according to the criteria

Table 12
Systematic and critical evaluation of the articles of Group 1 (IC-DV) according to the criteria specified in Section 5.1. See definition of numeration (1) to (14) in Table 8.

Group 1 Article	Main author	Research group	Country	Available online	Journal	# cits.	Evaluation criteria 1	2	3	4	5	6	7	8	9	10	11	12	13	14
[10]	Dubarry	HNEI	USA	Jul-12	JPS	206	Y	Y	Y	Y	Y	pOCV &IC-DV	LFP	CAL	Off&On	n.a.	NEV	Y	NEV	NEV
[43]	Devie	HNEI	USA	Mar-15	ECS	21	Y	Y	Y	Y	NEV	pOCV &IC-DV	LTO&NMC	RS	Off&On	n.a.	NEV	Y	NEV	NEV
[44]	Berecibar	IKERLAN	Spain	Dec-16	IEEE	1	N	Y	N	N	N	IC	NMC	RS	Off&On	n.a.	NEV	NEV	NEV	NEV
[78]	Dubarry	HNEI	USA	May-17	JPS	10	Y	Y	Y	Y	Y	pOCV	LTO, NMC & LFP	RS	Off&On	n.a.	NEV	Y	NEV	NEV

Table 13
Systematic and critical evaluation of the articles of Group 2 (IC-DV) according to the criteria specified in Section 5.1. See definition of numeration (1) to (14) in Table 8.

Article	Main author	Research group	Country	Available online	Journal	# cits.	Evaluation criteria 1	2	3	4	5	6	7	8	9	10	11	12	13	14
[48]	Dubarry	HNEI	USA	Feb-14	JPS	73	Y	Y	Y	Y	NEV	pOCV &PA	LFP	CAL	Off&On	S	NEV	Y	NEV	NEV
[49]	Anseán	Univ. of Oviedo	Spain	May-2016	JPS	32	Y	Y	Y	Y	NEV	pOCV &PA	LFP	RS	Off&On	n.a.	NEV	Y	NEV	NEV
[4]	Anseán	Univ. of Oviedo	Spain	Apr-2017	JPS	15	Y	Y	Y	Y	NEV	pOCV &PA	LFP	RDC	Off&On	n.a.	NEV	Y	NEV	NEV
[50]	Gao	Beijing Jiaotong Univ.	China	Apr-2017	JPS	17	Y	Y	Y	Y	NEV	pOCV &PA	LCO	RS	Off	n.a.	NEV	Y	NEV	NEV

specified in Section 5.1.

Pastor-Fernández et al. [51] use the conclusions derived from Dubarry et al. [10] to identify the DMs by means of full cell IC and DV curves. The authors used a metric called growth of degradation, G_{IC-DV}, to quantify the effects of DMs. This study uses the experimental data collected in Ref. [2] where four NCA-C Li-ion cells connected in parallel were cycled until their EoL. The results of this study agree with the outcomes obtained using the EIS technique in the same scenario as shown in Ref. [3]. The main contribution of [51] is the development of an automated method to quantify DMs based on full-cell IC-DV curves. The main limitation of this study is that the assumptions of which this approach is founded may not always be true. Further work includes validating this approach over a broader range of conditions.

5.3.4. Benefits and limitations of IC-DV techniques

Analysing Table 12, the advantages and disadvantages of the method of each Group are compared in Table 15 according to the requirements defined in Section 5.2. In case that not all the articles of a group fulfill a particular metric, the references of the articles that fulfill a specific metric is shown. It is seen that the methods of each group have approximately the same advantages and limitations. All three groups fulfill aspects (1–3) and (6), highlighting that they are automated, universal and suitable for identification of DMs. Group 2 and 3 have also the capability to quantify the DMs. However, as the main disadvantage, all three groups lack in an on-board implementation capability (5). In addition, they do not fulfill aspects 11, 13 and 14. Apart from these, Group 1 fulfills aspects number 9 and 12; Group 2 aspects 8, 9, 10 and 12; and Group 3 only 10. Hence, between the different groups, number 2 is the one which concentrates more advantages.

5.4. pOCV and IC-DV studies focus on on-board implementation and battery pack scalability

There is a number of studies which applies pOCV and IC-DV techniques for SoH estimation rather than for quantification of DMs. Although they do not identify neither quantify DMs, it is noteworthy to mention them because some of their aspects can add value to the techniques described in Section 5.2 and Section 5.3. These complementary studies have been classified into two groups depending on the aspect that add value:

- **Group 1:** these studies [47,79–81] support the capability of pOCV and IC-DV methods to be implemented on-board within a commercially viable BMS.
- **Group 2:** these articles [82,83] contribute to scale pOCV and IC-DV techniques from cell to module and battery pack.

From this classification, the specific contribution of the articles of each group is summarised in Table 16. As these articles are not aimed to identify neither quantify DMs, it is beyond the scope of this study to review them in detail.

5.5. Electrochemical Impedance Spectroscopy (EIS)

Only the studies presented by Pastor-Fernández et al. [3,66] were found to be relevant in terms of automation, identification and quantification of DMs. Table 17 evaluates these studies according to the criteria specified in Section 5.1.

Pastor-Fernández et al. [66] proposes to track the change of the EIS spectrum through the AR-ECM resistances (ohmic, SEI, charge-transfer and Warburg) so that DMs are quantified. The main limitation of this study is the lack of validation though e.g., post-mortem analysis. In addition, the challenges to implement EIS measurement within a battery pack need to be studied.

5.6. Combination of thermodynamic (pOCV) and kinetic (EIS) methods

Only the research presented by Schindler et al. [20] combines a thermodynamic (pOCV) and a kinetic (EIS) method to identify and quantify DMs following an automated process. Table 18 evaluates this study according to the criteria specified in Section 5.1.

Schindler et al. [20] identify and quantify the DMs based on the fusion of an overpotential (pOCV) and a kinetic (EIS) model. The results of the overpotential model show a linear dependency between relative R_{ohm} and LLI values, and R_{pol} and LAM values. Further experimental work involving different cell chemistry types and testing conditions (C-rate, SoC and temperature) need to be performed in order to validate this linear relationship.

5.7. Differential Thermal Voltammetry (DTV)

Table 19 evaluates the DTV articles found in the literature according

Table 14
Systematic and critical evaluation of the articles of Group 3 (IC-DV) according to the criteria specified in Section 5.1. See definition of numeration (1) to (14) in Table 8.

Article	Main author	Research group	Country	Available online	Journal	# cits.	Evaluation criteria 1	2	3	4	5	6	7	8	9	10	11	12	13	14
[51]	Pastor-Fernández	WMG	UK	Nov-16	IEEE	4	Y	Y	Y	Y	NEV	IC-DV	NCA	RS	Off	S	NEV	NEV	NEV	NEV
[3]	Pastor-Fernández	WMG	UK	Jun-17	JPS	8	Y	Y	Y	Y	NEV	IC-DV	NCA	RS	Off	S	NEV	NEV	NEV	NEV

Table 15
Comparison of the benefits and limitations of the of Group 1, 2 and 3 IC-DV methods according to the evaluation criteria described in Section 5.1.

Group	Evaluation criteria														Key
	1	2	3	4	5	6	7	8	9	10	11	12	13	14	articles
Group 1 [10,43,44,78]	✓ [10,43,78]	✓ [All]	✓ [10,78]	✓ [10,43,78]	✗	✓ [All]	✓ [43,78]	✗	✓ [All]	✗	✗	✓ [10,43,78]	✗	✗	[10]
Group 2 [4,48–50]	✓ [All]	✓ [All]	✓ [All]	✓ [All]	✗	✓ [4,48,49]	✗	✓ [4]	✓ [4,48,49]	✓ [48]	✗	✓ [All]	✗	✗	[48]
Group 3 [3,51]	✓ [All]	✓ [All]	✓ [All]	✓ [All]	✗	✓ [All]	✗	✗	✗	✓ [All]	✗	✗	✗	✗	[51]

Table 16
Systematic and critical evaluation of the articles focus on on-board implementation according to the criteria specified in Section 5.1. See definition of numeration (1) to (14) in Table 8.

Group 1																					
Article	Main author	Research group	Country	Available online	Journal	# cits.	Evaluation criteria 1	2	3	4	5	6	7	8	9	10	11	12	13	14
[47]	Feng	Tsinghua Uni.	China	Jan-13	JPS	63	N	N	N	N	Y	IC&DV	LFP& LMO	RS	On	n.a.	2% SoH_{est}	N	N	NEV
[79]	Weng	Uni. of Michigan	USA	Feb-13	JPS	120	N	N	N	N	Y	pOCV&IC	LFP	RS	Off&On	S (187s)	1% 1C	Y	NEV	NEV
[80]	Riviere	EVE System	France	Dec-15	IEEE	9	N	N	N	N	Y	IC	LFP	RS	Off&On	n.a.	2% SoH_{est}	NEV	NEV	NEV
[81]	Wang	Jiangsu & Shandong Uni.	China	Feb-16	AE	25	N	N	N	Y	Y	DV	LFP	RS	Off&On	S (17 ms)	2.5% SoH_{est}	Y	Y	NEV
Group 2																				
Article	**Main author**	**Research group**	**Country**	**Available online**	**Journal**	**# cits.**	**Evaluation criteria 1**	**2**	**3**	**4**	**5**	**6**	**7**	**8**	**9**	**10**	**11**	**12**	**13**	**14**
[82]	Zheng	Tsinghua Uni.	China	Dec-14	JPS	27	Y	Y	N	Y	NEV	ECDS	LFP	RS	Off&On	n.a.	0.03 Ah	NEV	Y	NEV
[83]	Weng	Michigan & Tsinghua Uni.	China	Aug-16	AE	31	N	N	N	Y	Y	pOCV &IC	LFP	RS	Off&On	n.a	in C 1.62% SoH_{est}	Y	Y	NEV

to the criteria specified in Section 5.1.

Wu et al. [17] present the DTV as a diagnostic technique to identify ageing mechanisms using voltage and temperature measurements in galvanostatic mode. The main limitation of this study is that the identification of the ageing mechanisms does not follow an automated approach and therefore, they are subject to different interpretations. To avoid this, Merla et al. [18] proposed peak position, peak width and peak height as FOIs of DTV curves to analyse the ageing mechanisms in an automated way. The results showed that it is challenging to predict the ageing mechanisms involved through individual peak parameter observation. Although the peak and changes of the DTV curves can be used to infer DMs, this result shows clearly in practice is not possible. Another common limitation of [17,18] is that the DTV was validated on individual cells under natural convection thermal boundary conditions. Merla et al. [19] used DTV to identify the ageing mechanisms of four commercial NMC connected in parallel placed under forced air surface cooling to emulate a BEV application. One of the cells was aged on purpose to demonstrate the diagnosis capability of the DTV. Despite this, the DTV results obtained for the four cells in parallel were comparable to the results obtained for the single cell test under natural convection [18]. From the same research group as [17–19], the last DTV study was published by Shibagaki et al. [69]. Following on from the same model as in Refs. [17–19], Shibagaki et al. [69] correlate peak DTV curve parameters with capacity fade, resistance increase and inhomogeneous electrode performance suggesting that the technique could be used for SoH estimation in real applications.

5.8. Comparison, benefits and limitations of diagnosis techniques

According to the criterion specified in Section 5.1, 14 different metrics were used to review the articles of each diagnostic technique. In addition to these metrics, other figures were evaluated to have a better understanding of the research groups involved in this field and the impact of their publications (refer to Section 5.1). This “soft” data and the scientific data (14 evaluation metrics) are treated separately. Fig. 10 illustrates the level and the spread of the activity of different groups in

Table 17
Systematic and critical evaluation of the EIS related articles according to the criteria specified in Section 5.1. See definition of numeration (1) to (14) in Table 8.

Article	Main author	Research group	Country	Available online	Journal	# cits.	Evaluation criteria 1	2	3	4	5	6	7	8	9	10	11	12	13	14
[66]	Pastor-Fernández	WMG	UK	Jul-16	IEEE	4	Y	Y	Y	NEV	NEV	EIS	NCA	RS	Off	S	10% in R in R	NEV	NEV	NEV
[3]	Pastor-Fernández	WMG	UK	Jun-17	JPS	8	Y	Y	Y	NEV	NEV	EIS	NCA	RS	Off	S	10% in R in R	NEV	NEV	NEV

Table 18
Systematic and critical evaluation of the combination article (pOCV + EIS) according to the criteria specified in Section 5.1. See definition of numeration (1) to (14) in Table 8.

Article	Main author	Research group	Country	Available online	Journal	# cits.	Evaluation criteria 1	2	3	4	5	6	7	8	9	10	11	12	13	14
[20]	Schindler	ZSW	Germany	Jan-17	JPS	5	Y	Y	Y	Y	NEV	pOCV & EIS	LFP	RS	Off&On	n.a.	1% in pOCV	NEV	NEV	NEV

Table 19
Systematic and critical evaluation of the DTV articles according to the criteria specified in Section 5.1. See definition of numeration (1) to (14) in Table 8.

Article	Main author	Research group	Country	Available online	Journal	# cits.	Evaluation criteria 1	2	3	4	5	6	7	8	9	10	11	12	13	14
[17]	Wu	Imperial College London (ICL)	UK	Sep-14	JPS	29	N	N	N	Y	NEV	SRCV, IC EIS & DTV	NMC	RS	Off	n.a.	NEV	Y	NEV	NEV
[18]	Merla	ICL	UK	Jan-16	JPS	22	N	N	N	Y	NEV	SRCV, IC EIS & DTV	NMC	RS	Off	n.a.	NEV	Y	NEV	NEV
[19]	Merla	ICL	UK	Sep-16	JPS	8	N	N	N	Y	NEV	SRCV, IC EIS & DTV	NMC	RS	Off	n.a.	NEV	Y	Y	NEV
[69]	Offer	ICL	UK	Nov-17	JPS	1	N	N	N	Y	NEV	DTV	LFP	RS	Off	n.a.	NEV	Y	Y	NEV

this research area.

From analysing Fig. 10 the following conclusions have been derived:

Fig. 10 **(a):** the techniques with a larger number of articles published are clearly pOCV (13) and IC-DV (10) followed by DTV (4), EIS (2) and Comb (1).• **Fig. 10 (b):** considering the affiliation of the first author in each publication, the most relevant research groups in the field are Tsinghua University (China) for pOCV, HNEI (USA) and University of Oviedo (Spain) for IC-DV, WMG (UK) for EIS, ZSW (Germany) for Comb. And Imperial College London (UK) for DTV.• **Fig. 10 (c):** from 2016 the topic of this study has acquired more importance in the literature for each of the techniques evaluated.• **Fig. 10 (d):** JPS is the journal which with more published articles related to these diagnostic techniques. Other journals or conference proceedings where these type of studies are published are AE, ECS, JPC, ASME, and IEEE.• **Fig. 10 (e):** the articles related to the pOCV technique are the most cited in the literature (737) followed by the IC-DV articles (387). In general, the articles related to the rest of the techniques (EIS, Comb. And DTV) are quite new, and hence, they have not been cited at that level.

According to Table 8, Table 12, Table 17, Tables 18 and 19, the 14 metrics defined in Section 5.1 were analysed with respect to the diagnostic techniques studied (pOCV, IC-DV, EIS, Combination (Comb.) and DTV). The results are illustrated in form of bar plots in Fig. 11. From these plots, conclusions are derived and summarised in Table 20.

From this comparison and the individual review of each article conducted along this section, the main benefits and limitations of each technique are shown in Table 21. Taking into consideration the results

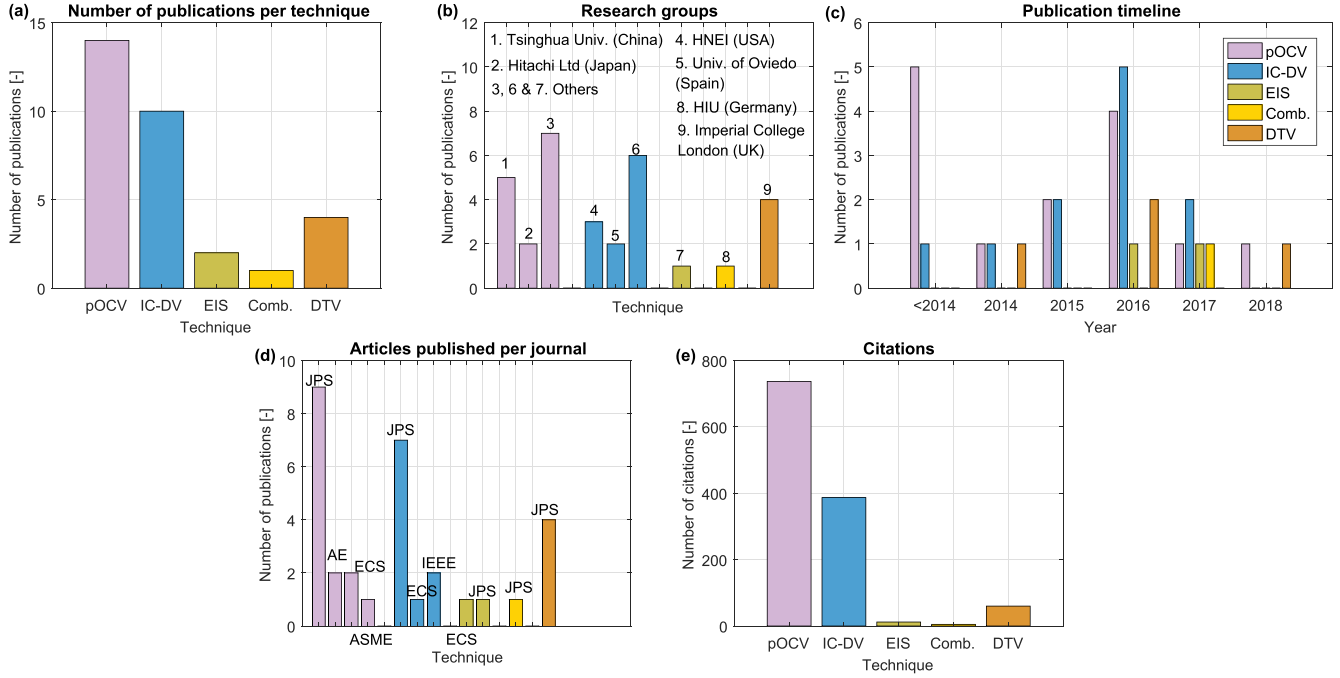

Fig. 10. Comparison of the soft metrics (a)–(i) between pOCV, IC-DV, EIS, Combination (Comb.) and DTV techniques: (a) number of articles published; (b) number of articles published by research group; (c) number of articles published per year; (d) number of articles published per journal and technique and (e) number of citations of the articles of each technique.

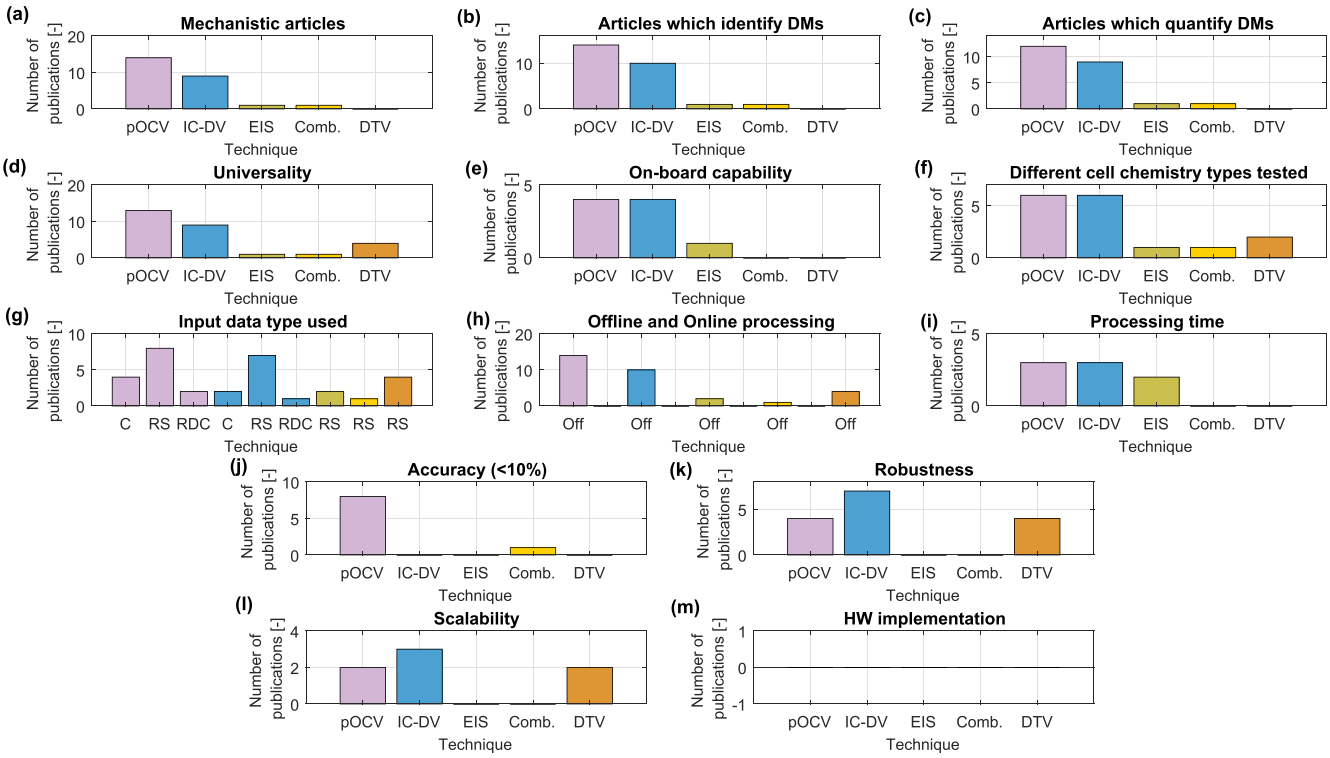

Fig. 11. Comparison of the scientific metrics: (a) number of articles which follow an automation process per technique; (b) number of articles per technique which identify DMs; (c) number of articles per technique which quantify DMs; (d) number of articles per technique which fulfills universality. (e) number of articles per technique which fulfills on-board capability; (f) number of different cell chemistry types tested per technique; (g) number of articles with respect to data type per technique; (h) number of articles in which the process is offline (Off), online (On), or offline and online (Off&On) per technique; (i) number of articles per technique in which the processing time is short (< 30min); (j) number of articles per technique in which the accuracy of the results is less than 10%; (k) number of articles per technique in which robustness is proved; (l) number of articles per technique in which scalability is proved; (m) number of articles per technique in which HW implementation is proved.

Table 20
Conclusions derived from comparing the reviewed non-invasive diagnostic techniques.

Figure	Conclusion
Fig. 11 (a)-(e)	For the analysis of the automation, identification, quantification, universality and on-board capability of each of the techniques there is a superior trend in the number of pOCV articles with respect to the IC-DV ones. Only the IC-DV technique seems to be advantageous in terms of on-board implementation. In comparison to the pOCV and IC-DV techniques, the rest of the techniques play a less significant role in these metrics. However, as a relative measure, all the EIS and Comb. reviewed articles fulfill the automation, identification and quantification (DMs) metrics. In contrast, the DTV technique only fulfills universality and on-board capability metrics.
Fig. 11 (f)	The number of different cell chemistry types tested is larger for the pOCV (LFP, LCO, NCO, LTO, LMO and NMC) and IC-DV (LFP, LTO, NMC, LCO and NCA) techniques than for the EIS (NCA), Comb. (LFP) and DTV (NMC) because the number of articles is also higher for these techniques.
Fig. 11 (g)	RS is the most common type of data used in all the techniques because it is easy to generate at laboratory conditions. The main disadvantage of this is that this type of data does not emulate real driving conditions (e.g., different C-rates, SoC, ΔDoD and temperature). Since the number of articles published is larger, pOCV and IC-DV techniques are also tested with C and RDC data.
Fig. 11 (h)	All the reviewed articles process the data offline.
Fig. 11 (i)	Only a few articles of the most published techniques (pOCV and IC-DV) provides a measure of the processing time. This result is because none of the reviewed studies attempt to implement the diagnostic methods into a real-time hardware environment. Then, the reported processing time is related to software based simulations, e.g., MATLAB based simulations.
Fig. 11 (j):	A measure of the accuracy is given in terms of error of pOCV estimation for the pOCV and Comb. (pOCV part) based methods. The accuracy is not evaluated in the studies reviewed for the rest of the methods. Therefore, the conclusions derived from these studies may not be 100% valid.
Fig. 11 (k)-(m)	Robustness and scalability are mainly proved for IC-DV and pOCV related articles, followed by the DTV ones. For both cases, the number of articles which fulfill these metrics is low as illustrates Fig. 10 (a). According to Fig. 11 (m), the HW implementation of the evaluated techniques has not been considered in the literature yet. This is because the research of these techniques is still in an early stage, and further work with this respect needs to be considered.

illustrated in Fig. 11 and the advantages and disadvantages listed in Table 21, it is seen that pOCV and IC-DV are the more advantageous techniques. However, these also lack in some aspects such as the necessity of acquiring accurate HC measurements and the duration of such experiment (> 10 h) or that the estimation of DMs may not be unique. Alternative techniques consider other ageing related parameters such as impedance (EIS) or temperature (DTV), or the combination of them (Comb.), which provide additional information to understand the DMs involved. These alternative techniques are not mature enough yet as they lack aspects such as on-board capability (EIS), robustness and scalability (EIS and Comb.), and capability to identify and quantify DMs (DTV). It is recommended therefore to use pOCV and IC-DV as reliable diagnostic techniques to identify and quantify DMs. At the same time, further developments of the alternative techniques (EIS, Comb. And DTV) need to be considered so that these techniques can contribute to understand better the diagnosis of DMs.

As suggested in our previous work [3], it is recommended to apply these techniques in an off-board environment (e.g., service station)

Table 21
Advantages and disadvantages of pOCV, IC-DV, EIS, Comb. And DTV diagnostic techniques.

Technique	Advantages	Disadvantages
pOCV	(a) Automated. (b) Identifies DMs. (c) Quantifies DMs. (d) Universal. (e) On-board capability. (f) Tested with RDC. (g) Accurate (< 10%). (h) Robust. (i) Scalable.	(a) Pristine HC-pOCV measurements are required at laboratory conditions. (b) pOCV test duration is long (> 10 h). (c) Ageing history measurements are required to discard the estimation of wrong DMs.
IC-DV	(a) Automated. (b) Identifies DMs. (c) Quantifies DMs. (d) Universal. (e) On-board capability. (f) Tested with RDC. (g) Robust. (h) Scalable.	(a) Pristine HC-pOCV measurements are required at laboratory conditions. (b) pOCV test duration is long (> 10 h). (c) Ageing history measurements are required to discard the estimation of wrong DMs. (d) Level of accuracy (< 10%) is not proved. (e) DMs can be neglected from the analysis of the IC-DV curves.
EIS	(a) Automated. (b) Identifies DMs. (c) Quantifies DMs. (d) Accurate (< 10%)	(a) Not mature technique for identification of DMs at laboratory conditions. (b) Universality is not proved. (c) On-board capability is not proved (HW implementation is complex). (d) Not tested with RDC input data. (e) Robustness is not proved. (f) Scalability is not proved.
Comb.	(a) Automated. (b) Identifies DMs. (c) Quantifies DMs. (d) Universal (thermodynamic model). (e) Accurate (< 10%).	(a) Pristine HC-pOCV measurements are required at laboratory conditions for the thermodynamic model. (b) Test duration is long (> 10 h) for pOCV test for the thermodynamic model. (c) Ageing history measurements are required to discard the estimation of wrong DMs. (d) Universality for the kinetic model is not proved. (e) On-board capability is not proved (HW implementation of the kinetic model is complex). (f) Not tested with RDC input data. (g) Robustness is not proved. (h) Scalability is not proved.
DTV	(a) Universal. (b) On-board capability. (c) Robust. (d) Scalable. (e) Entropic influence. (temperature) is considered. (f) Voltage can be measure up to 2C (faster than pOCV test in which the min C-rate is C/10).	(a) No automated. (b) No identifies DMs (only some ageing mechanisms). (c) No quantifies DMs (only some ageing mechanisms). (d) Level of accuracy (< 10%) is not proved. (e) Not tested with RDC input data.

rather than on-board. Two reasons support this recommendation:

1 HW implementation of these techniques is less limited off-board than on-board. In an off-board application, measurement outside the vehicle, there is access to more sophisticated equipment in terms e.g., speed, accuracy or precision, than in an on-board environment, where the characteristics of the HW components are more limited.

2 Under normal operation, degradation of LIBs is a slow process where significant changes can be noted after months or years. For instance, other functions such as voltage measurement need to be applied more quickly, e.g., in the order of milliseconds. This low frequent check suggests diagnosing DMs using external equipment (off-board).

6. Limitations of this study and further work

This review has highlighted that the most common limitations along the different techniques are:

- None of the reviewed techniques validates their results with post-mortem analysis.
- The conditions at which the techniques are tested (e.g., C-rate, SoC, ΔDoD or temperature) are repetitive following synthetic profiles rather than using more realistic profiles.
- Lack of on-board capability.
- Lack of scalability.
- Lack of HW implementation.

In addition, EIS, DTV and the combination of pOCV and EIS (Comb.) require improvements regarding robustness (refer to Table 21). In overall, DTV is the technique which requires more attention in the future since DTV does not fulfill the majority of the metrics (automation, identification of DMs, quantification of DMs, universality, accuracy level, robustness, scalability and HW implementation) included in the evaluation criterion.

From Section 5 it is seen that none of the diagnostic techniques proposed in the literature has been tested in real-world conditions within a vehicle. To do this, it is necessary to study the fundamental gap between the requirements of the diagnostic techniques (e.g., scalability or HW implementation) and the available functionalities of a commercial BMS. Further work includes the need to test these techniques in real-world conditions (off-board and on-board) to evaluate the level of accuracy and robustness required (e.g., in terms of sample rate or the level of noise immunity appropriate for the different diagnostic techniques). Such an experiment can be conducted using real-time hardware-in-the-loop systems. This would facilitate a level experimental

repeatability difficult to achieve within actual in-vehicle test.

7. Conclusions

In summary, this study comprises a critical review of the different techniques employed in the literature to quantify DMs. The outcomes of this study provide guidelines to select the most appropriate diagnostic techniques to identify and quantify DMs within different BMS applications.

The reviewed diagnostic methods are classified into thermodynamics based techniques (pOCV, IC-DV, and DTV), kinetics based (EIS) and a combination (Comb.) of them (pOCV + EIS). After an extensive review of the literature, these techniques are evaluated following the systematic criteria described in Section 5.1. In order to support the application of these methods in real-world scenarios, these criteria include requirements characteristics of the automotive domain. The results revealed that none of these techniques was tested in a vehicle in real-world conditions and thus, their hardware implementation requires further investigation. Furthermore, a practical application of these approaches may be more feasible off-board than on-board.

By comparing the different diagnostic techniques, pOCV and IC-DV are more advantageous than EIS, DTV and Comb. techniques because they fulfill a more significant number of requirements. Despite this, EIS, DTV and Comb. techniques employ different ageing indicators such as impedance for EIS, charge and impedance for Comb., and temperature for DTV. This result motivates the further evaluation of these techniques so that they can be implemented in real-world automotive applications in the future

Appendix A. Acknowledgments

The research presented within in paper is supported by the Engineering and Physical Science Research Council (EPSRC - EP/I01585X/1) through the Engineering Doctoral Centre in High Value, Low Environmental Impact Manufacturing. The research was undertaken in the WMG Centre High Value Manufacturing Catapult (funded by Innovate UK) in collaboration with Jaguar Land Rover. The authors would like also to thank Dr. Gael H. Chouchelamane for his support on the analysis of the results.

Appendix B. Nomenclature

Abbreviation

AE	Applied Energy
AR-ECM	Adapted Randles Equivalent Circuit Model
ARPA-E	Advanced Research Projects Agency for Energy
ASME	American Society of Mechanical Engineers
BMS	Battery Management System
CAL	Calendaric data
CF	Capacity Fade
CL	Conductivity Loss
Comb	Combination
DM	Degradation Modes
DoD	Depth of Discharge
DTV	Differential Thermal Voltammetry
EIS	Electrochemical Impedance Spectroscopy
FC	Full Cell
FOI	Feature of Interest
HC	Half Cell
HW	Hardware
HIU	Helmholtz-Institut Ulm
ICL	Imperial College London
IEEE	Institute of Electrical and Electronics Engineers
ISO	International Standard Organisation
JCP	Journal of Cleaner Production
JPS	Journal of Power Sources
L	Long (processing time)
LAM	Loss of Active Material
LCO	Lithium Cobalt Oxide ($LiCoO_2$)
LFP	Lithium iron Phosphate ($LiFePO_4$)
LIB	Lithium-ion Battery
LLI	Loss of Lithium Inventory
LMO	Lithium Manganese Oxide ($LiMn_2 O_4$)
LNO	Lithium Nickel Oxide ($LiNiO_2$)
LTO	Lithium-Titanate Oxide ($Li_4 Ti_5O_{12}$)
M	Mid (processing time)
MCU	Microcontroller Unit
MISRA	Motor Industry Software Research Association
N	No
n.a.	not available
NCA	Nickel Cobalt Aluminum Oxide (LiNixCo1-x-yAlyO2)
NE	Negative Electrode
NEV	Not Evaluated
NMC or NCM	Lithium Nickel Manganese Cobalt Oxide (Li[NiMnCo] O_2)
NQ	Not Quantified
Off	Offline
On	Online
PA	Peak Area
PE	Positive Electrode
PF	Power Fade
pOCV	Pseudo Open Circuit Voltage
PSO	Particle Swarm Optimisation
RDC	Repetitive Drive Cycle
RMSE	Root Mean Square Error
RS	Repetitive Synthetic data
SH	Short (processing time)
SEI	Solid Electrolyte Interphase
SEM	Scanning Electron Microscopy
SPI	Solid Permeable Interphase
SRCV	Slow Rate Cyclic Voltammetry
SoC	State of Charge
SoH	State of Health
SW	Software
T	Temperature
Univ	University
WMG	Warwick Manufacturing Group
XPS	X-Ray Photoelectron Spectroscopy
Y	Yes
ZSW	Zentrum für Sonnenenergie und Wasserstoff-Forschung

References

[1] Farmann A, Waag W, Marongiu A, Sauer DU. Critical review of on-board capacity estimation techniques for lithium-ion batteries in electric and hybrid electric vehicles. J Power Sources 2015;281:114–30. https://doi.org/10.1016/j.jpowsour.2015.01.129.

[2] Pastor-Fernández C, Bruen T, Widanage WD, Gama-Valdez MA, Marco J. A study of cell-to-cell interactions and degradation in parallel strings: implications for the battery management system. J Power Sources 2016;329:574–85. https://doi.org/10.1016/j.jpowsour.2016.07.121.

[3] Pastor-Fernández C, Chouchelamane GH, Widanage W, Marco J. A comparison between electrochemical impedance spectroscopy and incremental capacity-differential voltage as Li-ion diagnostic techniques to identify and quantify the effects of degradation modes within battery management systems. J Power Sources 2017;360:301–18. https://doi.org/10.1016/j.jpowsour.2017.03.042.

[4] Anseán D, Dubarry M, Devie A, Liaw BY, García VM, Viera JC, Gonzalez M. Operando lithium plating quantification and early detection of a commercial LiFePO4 cell cycled under dynamic driving schedule. J Power Sources 2017:36–46. https://doi.org/10.1016/j.jpowsour.2017.04.072.

[5] Vetter J, Novák P, Wagner MR, Veit C, Möller KC, Besenhard JO, Winter M, Wohlfahrt-Mehrens M, Vogler C, Hammouche A. Ageing mechanisms in lithium-ion batteries. J Power Sources 2005;147(1–2):269–81https://doi.org/10.1016/j.jpowsour.2005.01.006.

[6] Somerville L, Hooper MJ, Marco J, McGordon A, Lyness C, Walker M, Jennings P. Impact of vibration on the surface film of lithium-ion cells. 2017. https://doi.org/

10.3390/en10060741.
[7] Bruen T, Marco J. Modelling and experimental evaluation of parallel connected lithium ion cells for an electric vehicle battery system. J Power Sources 2016;310:91–101. https://doi.org/10.1016/j.jpowsour.2016.01.001.
[8] Rumpf K, Naumann M, Jossen A. Experimental investigation of parametric cell-to-cell variation and correlation based on 1100 commercial lithium-ion cells. J Energy Storage 2017;14:224–43. https://doi.org/10.1016/j.est.2017.09.010.
[9] Weicker P. A systems approach to Lithium-Ion mattery management. Artech House; 2014.
[10] Dubarry M, Truchot C, Liaw BY. Synthesize battery degradation modes via a diagnostic and prognostic model. J Power Sources 2012;219:204–16. https://doi.org/10.1016/j.jpowsour.2012.07.016.
[11] Birkl CR, Roberts MR, Mcturk E, Bruce PG, Howey DA. Degradation diagnostics for lithium ion cells. J Power Sources 2016;341:1–35. https://doi.org/10.1016/j.jpowsour.2016.12.011.
[12] Marongiu A, Nlandi N, Rong Y, Sauer DU. On-board capacity estimation of lithium iron phosphate batteries by means of half-cell curves. J Power Sources 2016;324:158–69. https://doi.org/10.1016/j.jpowsour.2016.05.041.
[13] Pastor-Fernández C, Chouchelamane GH, Widanage WD, Marco J. EngD submission 2 - a comparison between electrochemical impedance spectroscopy and incremental capacity -differential voltage as Li-ion diagnostic techniques to identify and quantify the effects of degradation modes within battery management systems PhD. thesis University of Warwick; 2017.
[14] Honkura K, Takahashi K, Horiba T. State analysis of lithium-ion batteries using discharge curves K. Honkura. ECS Transact 2008;13(19):61–73. https://doi.org/10.1149/1.3018750.
[15] Han X, Ouyang M, Lu L, Li J, Zheng Y, Li Z. A comparative study of commercial lithium ion battery cycle life in electrical vehicle: aging mechanism identification. J Power Sources 2014;251:38–54. https://doi.org/10.1016/j.jpowsour.2013.11.029.
[16] Ouyang M, Feng X, Han X, Lu L, Li Z, He X. A dynamic capacity degradation model and its applications considering varying load for a large format Li-ion battery. Appl Energy 2016;165:48–59. https://doi.org/10.1016/j.apenergy.2015.12.063.
[17] Wu B, Yufit V, Merla Y, Martinez-Botas RF, Brandon NP, Offer GJ. Differential thermal voltammetry for tracking of degradation in lithium-ion batteries. J Power Sources 2015;273:495–501. https://doi.org/10.1016/j.jpowsour.2014.09.127.
[18] Merla Y, Wu B, Yufit V, Brandon NP, Martinez-Botas RF, Offer GJ. Novel application of differential thermal voltammetry as an in-depth state-of-health diagnosis method for lithium-ion batteries. J Power Sources 2016;307:308–19. https://doi.org/10.1016/j.jpowsour.2015.12.122.
[19] Merla Y, Wu B, Yufit V, Brandon NP, Martinez-Botas RF, Offer GJ. Extending battery life: a low-cost practical diagnostic technique for lithium-ion batteries. J Power Sources 2016;331:224–31. https://doi.org/10.1016/j.jpowsour.2016.09.008.
[20] Schindler S, Danzer MA. A novel mechanistic modeling framework for analysis of electrode balancing and degradation modes in commercial lithium-ion cells. J Power Sources 2017;343:226–36https://doi.org/10.1016/j.jpowsour.2017.01.026.
[21] Waag W, Fleischer C, Sauer DU. Critical review of the methods for monitoring of lithium-ion batteries in electric and hybrid vehicles. J Power Sources 2014;258(0):321–39https://doi.org/10.1016/j.jpowsour.2014.02.064.
[22] Rezvanizaniani SM, Liu Z, Chen Y, Lee J. Review and recent advances in battery health monitoring and prognostics technologies for electric vehicle (EV) safety and mobility. 2014.
[23] Berecibar M, Gandiaga I, Villarreal I, Omar N, Van Mierlo J, Van den Bossche P. Critical review of state of health estimation methods of Li-ion batteries for real applications. Renew Sustain Energy Rev 2016;56:572–87. https://doi.org/10.1016/j.rser.2015.11.042.
[24] Ungurean L, Cârstoiu G, Micea MV, Groza V. Battery state of health estimation: a structured review of models, methods and commercial devices. Int J Energy Res 2016;31(August 2007):135–47. https://doi.org/10.1002/er.3598. arXiv:arXiv:1011.1669v3.
[25] Zhang J, Lee J. A review on prognostics and health monitoring of Li-ion battery. J Power Sources 2011;196(15):6007–14. https://doi.org/10.1016/j.jpowsour.2011.03.101.
[26] Krupa M. Methods of technical prognosis - review. Int Sci J 2013:20–3.
[27] Karami N, El-Sheikh H, Moubayed N. Evaluation study of different useful life estimation techniques of lithium-ion battery. 2016. p. 77–82. https://doi.org/10.1109/EECEA.2016.7470769.
[28] Wu L, Fu X, Guan Y. Review of the remaining useful life prognostics of vehicle lithium-ion batteries using data-driven methodologies. Appl Sci 2016;6(6):166. https://doi.org/10.3390/app6060166.
[29] Zhang Y, Wang C-Y. Cycle-life characterization of automotive lithium-ion batteries with LiNiO2 cathode. J Electrochem Soc 2009;156(7):A527–35. https://doi.org/10.1149/1.3126385.
[30] Uddin K, Perera S, Widanage W, Somerville L, Marco J. Characterising lithium-ion battery degradation through the identification and tracking of electrochemical battery model parameters. Batteries 2016;2(2):13. https://doi.org/10.3390/batteries2020013.
[31] Smith AJ, Burns JC, Xiong D, Dahn JR. Interpreting high precision coulometry results on Li-ion cells. J Electrochem Soc 2011;158(10):A1136–42. https://doi.org/10.1149/1.3625232.
[32] Dubarry M, Devie A, Liaw BY. The value of battery diagnostics and prognostics. J Energy Power Sources 2014;1(5):242–9.
[33] Wohlfahrt-Mehrens M, Vogler C, Garche J. Aging mechanisms of lithium cathode materials. J Power Sources 2004;127(1–2):58–64. https://doi.org/10.1016/j.jpowsour.2003.09.034.
[34] Agubra V, Fergus J. Lithium ion battery anode aging mechanisms. Materials 2013;6(4):1310–25. https://doi.org/10.3390/ma6041310.
[35] Kubiak P, Edström K, Morcrette M. Review on ageing mechanisms of different Li-ion batteries for automotive applications. 2012.
[36] Rahn C, Wang C-Y. Battery systems engineering. John Wiley & Sons, Ltd.; 2013.
[37] Feng X, Sun J, Ouyang M, He X, Lu L, Han X, Fang M, Peng H. Characterization of large format lithium ion battery exposed to extremely high temperature. J Power Sources 2014;272:457–67. https://doi.org/10.1016/j.jpowsour.2014.08.094.
[38] Ouyang M, Chu Z, Lu L, Li J, Han X, Feng X, Liu G. Low temperature aging mechanism identification and lithium deposition in a large format lithium iron phosphate battery for different charge profiles. J Power Sources 2015;286:309–20. https://doi.org/10.1016/j.jpowsour.2015.03.178.
[39] Yan D, Lu L, Li Z, Feng X, Ouyang M, Jiang F. Durability comparison of four different types of high-power batteries in HEV and their degradation mechanism analysis. Appl Energy 2016;179:1123–30. https://doi.org/10.1016/j.apenergy.2016.07.054.
[40] Honkura K, Takahashi K, Horiba T. Capacity-fading prediction of lithium-ion batteries based on discharge curves analysis. J Power Sources 2011;196(23):10141–7. https://doi.org/10.1016/j.jpowsour.2011.08.020.
[41] Dahn HM, Smith AJ, Burns JC, Stevens DA, Dahn JR. User-friendly differential voltage analysis freeware for the analysis of degradation mechanisms in Li-ion batteries. J Electrochem Soc 2012;159(9):A1405–9. https://doi.org/10.1149/2.013209jes.
[42] Hu C, Hong M, Li Y, Jeong H-l. On-board analysis of degradation mechanisms of lithium-ion battery using differential voltage analysis. Proc ASME 2016:1–9. International design engineering technical conferences and computers and information in engineering conference (2016).
[43] Devie A, Dubarry M, Liaw BY. Overcharge study in Li4Ti5O12 based lithium-ion pouch cell: I. Quantitative diagnosis of degradation modes. J Electrochem Soc 2015;162(6):A1033–40. https://doi.org/10.1149/2.0941506jes.
[44] Berecibar JVMM, Dubarry M, Omar N, Villarreal I. Degradation mechanism detection for NMC batteries based on Incremental Capacity curves. 2016. p. 1–12. Evs29.
[45] Zhang C, Yan F, Du C, Kang J, Turkson R. Evaluating the degradation mechanism and state of health of LiFePO4 lithium-ion batteries in real-world plug-in hybrid electric vehicles application for different ageing paths. Energies 2017;10(1):110. https://doi.org/10.3390/en10010110.
[46] Lu T, Luo Y, Zhang Y, Luo W, Yan L, Xie J. Degradation analysis of a lithium-ion battery with a blended electrode. J Electrochem Soc 2017;164(2):A295–303. https://doi.org/10.1149/2.1051702jes.
[47] Feng X, Li J, Ouyang M, Lu L, Li J, He X. Using probability density function to evaluate the state of health of LiFePO4 lithium-ion batteries. J Power Sources 2013;232:209–18. https://doi.org/10.1016/j.jpowsour.2013.01.018.
[48] Dubarry M, Truchot C, Liaw BY. Cell degradation in commercial LiFePO4 cells with high-power and high-energy designs. J Power Sources 2014;258:408–19. https://doi.org/10.1016/j.jpowsour.2014.02.052.
[49] Anseán D, Dubarry M, Devie A, Liaw BY, García VM, Viera JC, González M. Fast charging technique for high power LiFePO4 batteries: a mechanistic analysis of aging. J Power Sources 2016;321:201–9. https://doi.org/10.1016/j.jpowsour.2016.04.140.
[50] Gao Y, Jiang J, Zhang C, Zhang W, Ma Z, Jiang Y. Lithium-ion battery aging mechanisms and life model under different charging stresses. J Power Sources 2017;356:103–14. https://doi.org/10.1016/j.jpowsour.2017.04.084.
[51] Pastor-Fernández C, Widanage WD, Chouchelamane GH, Marco J. A SoH diagnosis and prognosis method to identify and quantify degradation modes in Li-ion batteries using the IC/DV technique. 2016. https://doi.org/10.1049/cp.2016.0966.
[52] Sarasketa-Zabala E, Aguesse F, Villarreal I, Rodriguez-Martinez LM, López CM, Kubiak P. Understanding lithium inventory loss and sudden performance fade in cylindrical cells during cycling with deep-discharge steps. J Phys Chem C 2015;119(2):896–906. https://doi.org/10.1021/jp510071d.
[53] Abraham DP, Poppen SD, Jansen AN, Liu J, Dees DW. Application of a lithium–tin reference electrode to determine electrode contributions to impedance rise in high-power lithium-ion cells. Electrochim Acta 2004;49(26):4763–75. https://doi.org/10.1016/j.electacta.2004.05.040.
[54] Zhang S, Xu K, Jow T. Electrochemical impedance study on the low temperature of Li-ion batteries. Electrochim Acta 2004;49(7):1057–61. https://doi.org/10.1016/j.electacta.2003.10.016.
[55] Tröltzsch U, Kanoun O, Tränkler H-R. Characterizing aging effects of lithium ion batteries by impedance spectroscopy. Electrochim Acta 2006;51(8–9):1664–72. https://doi.org/10.1016/j.electacta.2005.02.148.
[56] Aurora P, Ramaswamy N, Han T. Electrochemical impedance spectroscopic analysis of lithium-ion battery aging mechanisms. ECS Transact 2010;147(2005):2013.
[57] Liu P, Wang J, Hicks-Garner J, Sherman E, Soukiazian S, Verbrugge M, Tataria H, Musser J, Finamore P. Aging mechanisms of LiFePO4 batteries deduced by electrochemical and structural analyses. J Electrochem Soc 2010;157(4):A499–507. https://doi.org/10.1149/1.3294790.
[58] Stiaszny B, Ziegler JC, Krauß EE, Schmidt JP, Ivers-Tiffée E. Electrochemical characterization and post-mortem analysis of aged LiMn2O4–Li(Ni0.5Mn0.3Co0.2)O2/graphite lithium ion batteries. Part I: cycle aging. J Power Sources 2014;251:439–50https://doi.org/10.1016/j.jpowsour.2013.11.080.
[59] Stiaszny B, Ziegler JC, Krauß EE, Zhang M, Schmidt JP, Ivers-Tiffée E. Electrochemical characterization and post-mortem analysis of aged LiMn2O4–NMC/graphite lithium ion batteries part II: calendar aging. J Power Sources 2014;258:61–75https://doi.org/10.1016/j.jpowsour.2014.02.019.
[60] Bauer M, Guenther C, Kasper M, Petzl M, Danzer MA. Discrimination of degradation processes in lithium-ion cells based on the sensitivity of aging indicators towards capacity loss. J Power Sources 2015. https://doi.org/10.1016/j.jpowsour.2015.02.130.

[61] Huhman BM, Heinzel JM, Mili L, Love CT, Wetz DA. Investigation into state-of-health impedance diagnostic for 26650 4P1S battery packs. J Electrochem Soc 2017;164(1):A6401–11. https://doi.org/10.1149/2.0631701jes.
[62] Schindler S, Bauer M, Petzl M, Danzer MA. Voltage relaxation and impedance spectroscopy as in-operando methods for the detection of lithium plating on graphitic anodes in commercial lithium-ion cells. J Power Sources 2016;304:170–80. https://doi.org/10.1016/j.jpowsour.2015.11.044.
[63] Howey D a, Mitcheson PD, Member S, Yufit V, Offer GJ, Brandon NP. Online measurement of battery impedance using motor controller excitation. IEEE Trans Veh Technol 2014;63(6):2557–66. https://doi.org/10.1109/TVT.2013.2293597.
[64] Din E, Schaef C, Member S, Moffat K, Member S, Stauth JT. A scalable active battery management system with embedded real-time electrochemical impedance spectroscopy. IEEE Trans Power Electron 2016;32:5688–98. https://doi.org/10.1109/TPEL.2016.2607519.
[65] Mingant R, Bernard J, Sauvant-Moynot V. Novel state-of-health diagnostic method for Li-ion battery in service. Appl Energy 2016;183:390–8. https://doi.org/10.1016/j.apenergy.2016.08.118.
[66] C. Pastor-Fernández, D. W. Widanage, J. Marco, M.-Á. Gama-Valdez, G. H. Chouchelamane, Identification and quantification of ageing mechanisms in lithium-ion batteries using the EIS technique, IEEE transportation electrification conference manuscript.
[67] Reynier YF, Yazami R, Fultz B. Thermodynamics of lithium intercalation into graphites and disordered carbons. J Electrochem Soc 2004;151(3):A422–6. https://doi.org/10.1149/1.1646152.
[68] Maher K, Yazami R. A study of lithium ion batteries cycle aging by thermodynamics techniques. J Power Sources 2014;247:527–33https://doi.org/10.1016/j.jpowsour.2013.08.053.
[69] Shibagaki T, Merla Y, Offer GJ. Tracking degradation in lithium iron phosphate batteries using differential thermal voltammetry. J Power Sources 2018;374(October 2017):188–95. https://doi.org/10.1016/j.jpowsour.2017.11.011.
[70] Ward D. MISRA standards for automotive software. 2nd IEE conference on automotive electronics 2006. p. 5–18. https://doi.org/10.1049/ic:20060570.
[71] Behkamal B, Kahani M, Akbari MK. Customizing ISO 9126 quality model for evaluation of B2B applications. Inf Softw Technol 2009;51(3):599–609. https://doi.org/10.1016/j.infsof.2008.08.001.
[72] Bosch GmbH Robert. Bosch automotive handbook. ninth ed. 2014.
[73] Dubarry M, Vuillaume N, Liaw BY. From single cell model to battery pack simulation for Li-ion batteries. J Power Sources 2009;186(2):500–7. https://doi.org/10.1016/j.jpowsour.2008.10.051.
[74] Tranfield D, Denyer D, Smart P. Towards a methodology for developing evidence-informed management knowledge by means of systematic review *. Br J Manag 2003;14:207–22. https://doi.org/10.1111/1467-8551.00375. arXiv:9605103.
[75] Denyer D, Tranfield D. Producing a literature review. SAGE handbook of organizational research methods. London: SAGE Publications Ltd.; 2009. Ch. 39.
[76] Google Inc. Google Scholar URL https://scholar.google.co.uk/, Accessed date: 8 July 2018.
[77] Ma Z, Wang Z, Xiong R, Jiang J. A mechanism identification model based state-of-health diagnosis of lithium-ion batteries for energy storage applications. J Clean Prod 2018;193:379–90. https://doi.org/10.1016/j.jclepro.2018.05.074.
[78] Dubarry M, Berecibar M, Devie A, Anseán D, Omar N, Villarreal I. State of health battery estimator enabling degradation diagnosis: model and algorithm description. J Power Sources 2017;360:59–69. https://doi.org/10.1016/j.jpowsour.2017.05.121.
[79] Weng C, Cui Y, Sun J, Peng H. On-board state of health monitoring of lithium-ion batteries using incremental capacity analysis with support vector regression. J Power Sources 2013;235:36–44. https://doi.org/10.1016/j.jpowsour.2013.02.012.
[80] E. Riviere, P. Venet, A. Sari, F. Meniere, Y. Bultel, U. Claude, B. Lyon, U. D. Lyon, V. Cedex, LiFePO 4 battery state of health online estimation using electric vehicle embedeed incremental capacity analysisdoi:10.1109/VPPC.2015.7352972.
[81] Wang L, Pan C, Liu L, Cheng Y, Zhao X. On-board state of health estimation of LiFePO4 battery pack through differential voltage analysis. Appl Energy 2016;168:465–72. https://doi.org/10.1016/j.apenergy.2016.01.125.
[82] Zheng Y, Ouyang M, Lu L, Li J. Understanding aging mechanisms in lithium-ion battery packs: from cell capacity loss to pack capacity evolution. J Power Sources 2015;278:287–95. https://doi.org/10.1016/j.jpowsour.2014.12.105.
[83] Weng C, Feng X, Sun J, Peng H. State-of-health monitoring of lithium-ion battery modules and packs via incremental capacity peak tracking. Appl Energy 2016;180:360–8. https://doi.org/10.1016/j.apenergy.2016.07.126.